NOAA Technical Report NOS CS 31

THE DESIGN, CALIBRATION AND VALIDATION OF A COUPLED NUMERICAL OCEAN MODELING SYSTEM FOR THE WEST FLORIDA SHELF

Silver Spring, Maryland
May 2011

noaa National Oceanic and Atmospheric Administration

U.S. DEPARTMENT OF COMMERCE
National Ocean Service
Coast Survey Development Laboratory

Office of Coast Survey
National Ocean Service
National Oceanic and Atmospheric Administration
U.S. Department of Commerce

The Office of Coast Survey (OCS) is the Nation's only official chartmaker. As the oldest United States scientific organization, dating from 1807, this office has a long history. Today it promotes safe navigation by managing the National Oceanic and Atmospheric Administration's (NOAA) nautical chart and oceanographic data collection and information programs.

There are four components of OCS:

The Coast Survey Development Laboratory develops new and efficient techniques to accomplish Coast Survey missions and to produce new and improved products and services for the maritime community and other coastal users.

The Marine Chart Division acquires marine navigational data to construct and maintain nautical charts, Coast Pilots, and related marine products for the United States.

The Hydrographic Surveys Division directs programs for ship and shore-based hydrographic survey units and conducts general hydrographic survey operations.

The Navigational Services Division is the focal point for Coast Survey customer service activities, concentrating predominately on charting issues, fast-response hydrographic surveys, and Coast Pilot updates.

NOAA Technical Report NOS CS 31

THE DESIGN, CALIBRATION AND VALIDATION OF A COUPLED NUMERICAL OCEAN MODELING SYSTEM FOR THE WEST FLORIDA SHELF

Lyon W. J. Lanerolle and Richard C. Patchen
Office of Coast Survey, Coast Survey Development Laboratory,
Silver Spring, MD

May 2011

noaa National Oceanic and Atmospheric Administration

U. S. DEPARTMENT OF COMMERCE
Gary Locke,
Under Secretary

National Oceanic and Atmospheric Administration
Dr. Jane Lubchenco
Administrator

National Ocean Service
David Kennedy
Assistant Secretary

Office of Coast Survey
Captain John Lowell, NOAA

Coast Survey Development Laboratory
Mary Erickson

NOTICE

Mention of a commercial company or product does not constitute an endorsement by NOAA. Use for publicity or advertising purposes of information from this publication concerning proprietary products or the tests of such products is not authorized.

.

TABLE OF CONTENTS

LIST OF FIGURES

LIST OF TABLES

EXECUTIVE SUMMARY

Global and basin-scale numerical ocean models run on model grids which are too coarse to resolve most bays and estuaries. Conversely, using bay and estuary resolving grids with such models would produce grids with prohibitively large numbers of grid points and the time step restrictions for running on such grids would be unacceptably strict. Therefore, model coupling (or nesting) is a reasonable way to downscale global/basin-scale models to perform high resolution computations in localized regions. Model coupling can be carried out either as a two-way nesting within the same model or by coupling two separate models sharing common interfaces through which model boundary information is passed. Due to the greater degree of flexibility associated with the latter, it is often preferred and this approach is also adopted in the present research. In this report, a ROMS-based high resolution model (NWFS-3D) for the west Florida shelf (WFS) is coupled to a POM-based, basin-scale Gulf of Mexico model (NGOM). The coupling is effected through the initialization fields and the lateral and surface boundary condition fields all of which are interpolated on to the NWFS-3D model grid from the NGOM grid. A specific boundary condition treatment for the barotropic velocities was necessary to alleviate the entrapment of barotropic waves within the NWFS-3D model domain and allowed them to be freely transmitted in and out of it. The model coupling was calibrated and validated through a 15-day NWFS-3D simulation after its bathymetry and coastline had been replaced with those of the lower resolution NGOM model. A comparison of the water elevations, currents, temperature and salinity showed that NWFS-3D was able to faithfully reproduce the corresponding fields from NGOM. The coupled system was then employed to perform a 6-month synoptic hindcast simulation from June 15, 2005 to December 15, 2005 for which NGOM model output fields and observed data were available. This period also included the presence of five hurricanes (Dennis, Emily, Katrina, Rita, Wilma) which enabled the numerical stability, robustness and reliability of the coupled system to be severely tested. Comparisons of the NWFS-3D water elevation, currents, temperature and salinity fields with observations showed that they were in good general agreement with each other and within the NOAA/NOS skill assessment standards – that is, within 15 cm for water elevation amplitudes, 26 cm/s for currents speeds, 2^{o}C for temperature and 3.5 PSU for salinity. The NWFS-3D predictions were consistent with those of NGOM as well. Extension of this research effort could involve : (i) re-running the synoptic hindcast simulation with a range of surface forcing meteorological products (for example, those from the Global Forecast System (GFS), the North American Regional Renalysis (NARR) model, the National Digital Forecast Database (NDFD), etc.) to possibly further improve the NWFS-3D model predictions and obtain ensemble predictions and (ii) the operational implementation of the NWFS-3D set-up to run in real-time and generate daily model forecasts for the WFS region. The coupling methodology designed and proven in this report are sufficiently general and flexible that they are not restricted to modeling applications in WFS region only but are generally applicable to any region around the world.

1. INTRODUCTION AND MOTIVATION

Global and basin-scale numerical ocean models run on model grids with spatial grid resolutions of 5 km or greater. At such resolutions, it is impossible to resolve bays, estuaries and embayments sufficiently. If however, these models are operated at spatial resolutions capable of resolving bays, estuaries and embayments, the model grids will have a prohibitively large number of grid points, to be run even on a supercomputer, with a suitable parallelization mode such as Message Passing Interface (MPI) or Open Multi-Processing (OpenMP), in a reasonable amount of time. Furthermore, the time-step restrictions for numerical stability of such models will be dictated by the smallest of the spatial scales and thus the time-stepping procedure will be too time consuming. Moreover, using excessively fine grid spacings and time-steps in regions for which there is no such necessity would constitute a waste of computational effort.

Therefore, it would be reasonable to couple/nest spatio-temporally high resolution local or regional models to the larger global or basin-scale models where the former would be used to cover individual bays and estuaries to resolve their physics sufficiently. The model surface and lateral boundary forcing for the local/regional models can be derived from the global/basin-scale models which could also provide any necessary initial conditions and river forcing fields.

Model coupling can be achieved in two ways : (i) via a two-way nesting procedure within the same model (Debreau and Balyo, [2009], Sheng, et.al, [2005], Blayo and Debreu, [2006]) or (ii) by coupling two different numerical ocean models sharing common interfaces (Weisberg, et. al, [2009], Alvera and Barth, [2009], Zavatarelli and Pinardi, [2003], Kourafalou and Tsiaras, [2007]). In addition to the fact that two-way nesting algorithms still have not reached full maturity in the field of numerical ocean modeling, (ii) has the specific advantages that : (a) a reliable technology to carry out this coupling is currently available, (b) it allows the use of different numerical ocean models (if necessary) for the global/basin-scale and nested/coupled domains whereby an improved model can be used for the latter and the user is not limited by the former, (c) the forcings associated with the nested/coupled domain can be refined or modified according to need and (d) the physical processes to be modeled within the nested/coupled domain are not limited by those of the global/basin-scale domain and different or additional physical processes can be included in the former – for example, non-hydrostatic effects, sediment transport, the use of a different vertical eddy-viscosity formulation, data assimilation, etc. Therefore, option (ii) gives the user a greater degree of flexibility and this is also the approach adopted in the present research. Hereafter, the term nested will be omitted and the term coupled will be used consistently throughout the remainder of this report.

In the present research, a shelf-scale Rutgers University's Regional Ocean Modeling System (ROMS) model is coupled to a basin-scale Princeton Ocean Model (POM) model. ROMS is a split-explicit, finite difference based orthogonal, curvilinear grid numerical ocean model (Shchepetkin and McWilliams, 2004). The vertical grid is of a stretched, terrain-following, sigma coordinate (Song and Haidvogel, 1994) type. The momentum and tracer advection terms are discretized using high resolution, third order upstream-biased advection schemes which alleviate the need to add explicit horizontal viscosity/diffusivity in the numerical computations (Shchepetkin and McWilliams, 1998). The hydrostatic pressure gradient terms are also discretized using an extremely robust and accurate piecewise cubic spline construction

(Shchepetkin and McWilliams, 2003). The vertical turbulence/eddy mixing is carried out using a standard Mellor-Yamada 2.5 scheme (Mellor and Yamada, 1982), a non-local K-Profile Parameterization (KPP) scheme or a family of General Length Scale (GLS) schemes consisting of k-ε, k-τ and k-ω schemes (Warner et. al., 2005). Along the ocean bottom bathymetry, friction can be prescribed with a logarithmic, linear, quadratic law or a Bottom Boundary Layer (BBL) formulation (Styles and Glenn, 2000). At the ocean surface, the surface meteorological forcing can be imposed in two ways in ROMS – *(a)* if the wind stresses and net heat fluxes are available then, they can be prescribed directly but otherwise, *(b)* the wind speeds, air pressure, air temperature, relative humidity, net shortwave radiation flux and downward longwave radiation flux observations when available are specified and then the wind stresses and the net heat flux are estimated internally using a Bulk Flux formulation (Liu et. al, 1979; Fairall et. al, 1996a,b). If downward longwave radiation data is unavailable, the net longwave radiation can be computed internally using the Berliand formulation (Berliand and Berliand, 1952). The perfect restart mechanism contained in the ROMS allows lengthy computations to be carried out in reasonably sized run segments.

The POM application covers the whole of the Gulf of Mexico and as far as 78^{o} W in to the Atlantic ocean and the region between the 18^{o} N and 31^{o} N latitudes. The nominally 5 km resolution POM model application is called the National Oceanographic and Atmospheric Administration (NOAA)/National Ocean Service (NOS) Gulf of Mexico (NGOM) model. The coupled ROMS domain covers the west Florida shelf from just north of Tampa Bay to just south of Cape Romano, FL and out to the 100m isobaths on the shelf. This coupled ROMS application is called NOAA/NOS West Florida Shelf three dimensional (NWFS-3D) model and is of much higher spatial resolution than NGOM. The NGOM domain does not include Tampa Bay and Charlotte Harbor but they are included in the NWFS-3D domain.

The NWFS-3D model was initialized and forced (surface, lateral and river forcings) using fields interpolated from the larger, NGOM model. For initialization, water elevation, temperature and salinity fields were employed and the model was spun-up from rest. The surface forcing used interpolated wind stresses and (monthly climatological) net heat fluxes. The lateral boundary forcing employed water elevation, velocity, temperature and salinity fields. The river forcing was done with river volume discharges, river temperatures and salinities. The NWFS-3D – NGOM coupled system was calibrated and validated with a 15-day simulation using the low-resolution NGOM bathymetry and coastline and then, ensuring that it was able to reproduce the NGOM flow-fields (water elevations, currents, temperature and salinity) sufficiently accurately. Thereafter, using the highest resolution bathymetry and coastline available. a 6-month synoptic hindcast simulation spanning June 15, 2005 – December 15, 2005 was performed and the model predictions (water elevations, currents, temperature and salinity) from NWFS-3D were evaluated against those of NGOM and also against observed data. This simulation period was selected due to the availability of NGOM fields, observational data and the presence of five hurricanes (Dennis, Emily, Katrina, Rita, Wilma) which served to test the numerical stability, robustness and reliability of the coupled system.

The contents of this report are arranged as follows. Section 2 describes the two coupling domains, their respective model grids and their bathymetries. In Section 3, the coupling methodology in terms of the initial, boundary and other compatibility conditions are explained.

The validation of the model coupling is documented in Section 4 and the results of the validation experiments are provided in Appendix A. The synoptic hindcast simulation is described in Section 5 and the model-observations comparisons are given in Appendix B and C. Finally, in Section 6 a summary, some conclusions and further directions regarding the present research are stated.

2. COUPLED DOMAINS, GRIDS AND BATHYMETRY

The basin-scale NGOM model domain and shelf-scale NWFS-3D sub-domain employed in the coupling are shown in Figure 1.

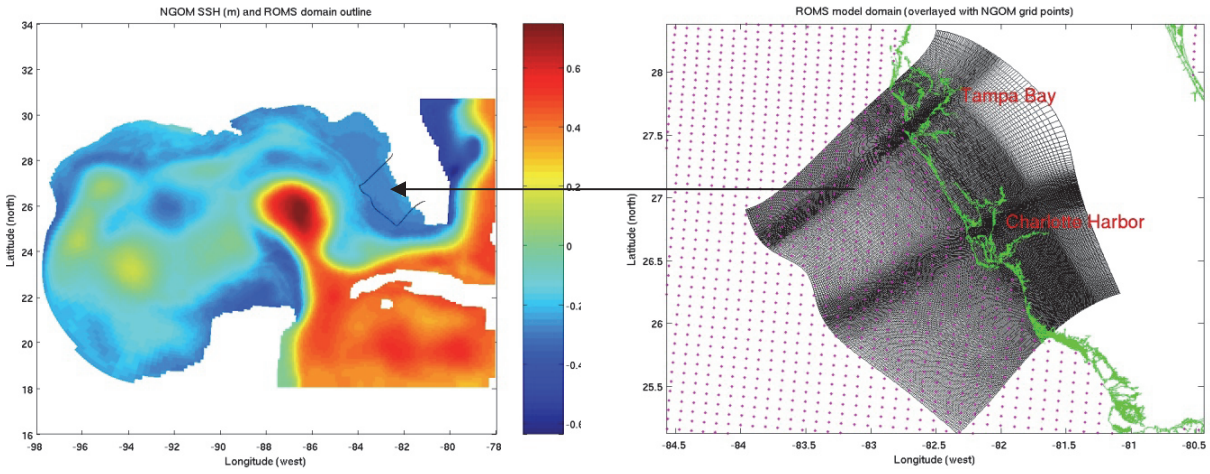

Figure 1. NGOM model domain with the NWFS-3D sub-domain (left) and NWFS-3D model grid (right). Red dots on the right figure indicate NGOM grid point locations.

The NGOM grid spacing is relatively uniform over the WFS area with a model resolution of ~5 km and it does not include Tampa Bay or Charlotte Harbor. The NWFS-3D grid was generated using the Matlab-based SeaGrid grid generating tool (SeaGrid, 2009) and it has 298 x 254 grid points in the horizontal and 30 model σ-levels in the vertical. It was made to conform to the medium resolution coastline product from NOAA/National Geophysical Data Center (NGDC). Tampa Bay and Charlotte Harbor were included as they bring in river discharges and hence also nutrients to the WFS region. The upper cross-shore (western) lateral boundary of the NWFS-3D grid is close to Palm Harbor, FL which is north of Tampa Bay and the lower cross-shore (eastern) lateral boundary is close to Marco, FL which is south of Charlotte Harbor. The along-shore (southern) lateral boundary follows the 100m isobath on the WFS. As shown in Figure 1, there are three regions of refinement in the NWFS-3D grid which are (i) Tampa Bay, (ii) Charlotte Harbor and (iii) the near-coastal zone (adjacent to the coast). This added refinement was incorporated in order to capture the physical processes which occur within these regions. Figure 2 shows the grids associated with (i) and (ii).

The grid resolution of the NWFS-3D grid is shown in Figure 3. In Tampa Bay and Charlotte Harbor it is ~400 m and a nominal value for the shelf is ~800m and is of much higher resolution on the WFS than its NGOM counterpart. Hence, the former is expected to be able to capture the fine-scale dynamics (e.g. eddies, etc.) which NGOM was not designed to account for.

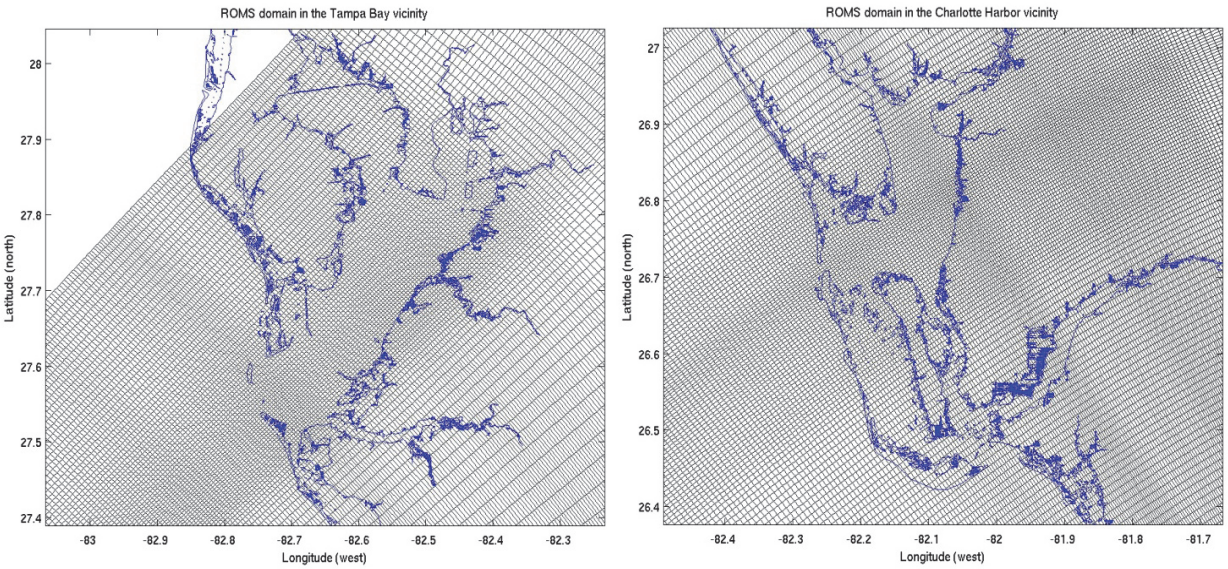

Figure 2. The NWFS-3D grid in the Tampa Bay (left) and Charlotte Harbor (right) regions.

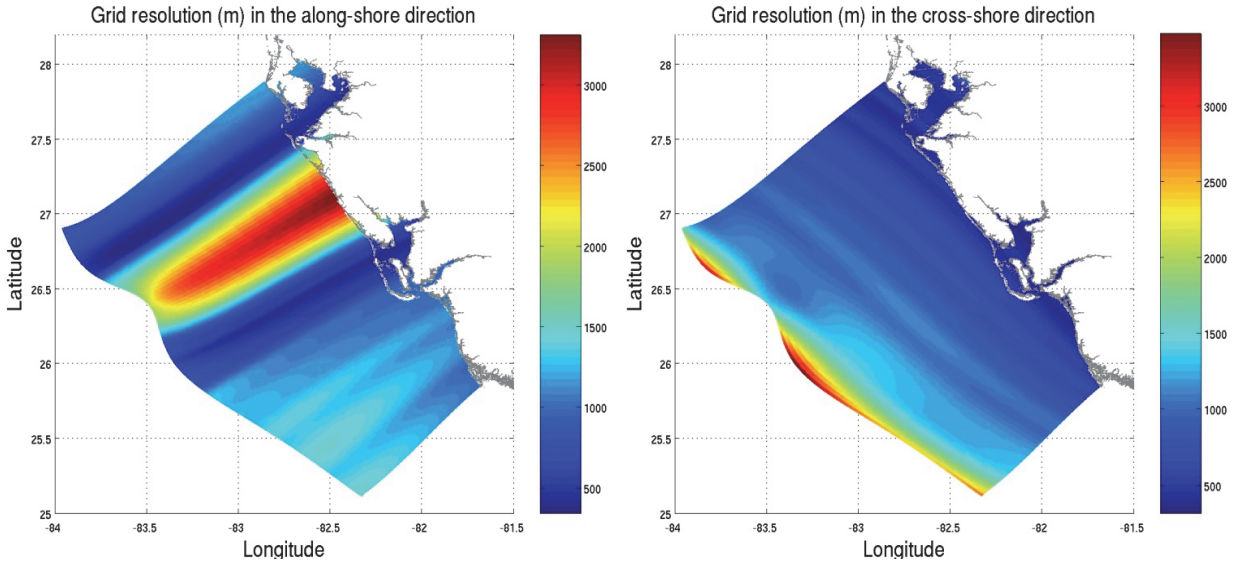

Figure 3. Along-shore (left) and cross-shore (right) grid resolution (m) for the NWFS-3D grid.

For both the NGOM and NWFS-3D grids, the bathymetry was derived from the NOAA/National Ocean Service (NOS) soundings. The soundings were interpolated on to the NWFS-3D grid nodes (at wet-points) using an inverse-square distance weighted numerical algorithm. All of the depths shallower than 2m were truncated to 2m which was also the depth associated with the land/dry points in the computational domain; neither the NGOM nor the NWFS-3D models had

their wetting-drying capabilities invoked as it was deemed not necessary. The bathymetry of the two domains is plotted in Figure 4 and they show the relatively higher resolution of the NWFS-3D grid especially in the near-coastal and shelf-break regions. Along the open ocean boundary of the NWFS-3D grid, its bathymetry matches the corresponding values on the NGOM grid and it was carried out in a smooth fashion over a distance of five grid points using a linear interpolation technique. The two bathymetries need to be reconciled at the NWFS-3D open boundaries in order to ensure that the volume transport exiting the NGOM domain is indeed that entering the NWFS-3D domain or else, mass, heat and salt conservation between the two domains would be violated.

In the vertical, an innovative terrain-following σ-grid formulation is used. In the shallow regions, a greater concentration of grid points is clustered near the bottom in order to resolve the bottom boundary layer. In the deeper regions, clustering occurs both near the bottom and also in the vicinity of the surface in order to resolve the bottom and surface boundary layers respectively.

This grid point distribution is brought about by the following depth-σ transformation where the true model depth, h which is a function of the vertical σ level and time, t is prescribed as:

$$h(\sigma, t) = z_0(\sigma) + \eta(t) \cdot [1 + z_0/H]$$

and, $z_0(\sigma) = (\sigma - C_\sigma) \cdot h_C + H \cdot C_\sigma$ and, $C_\sigma = -\left|\{1 - (1+\sigma)^{2\theta_s}\}^{\theta_b}\right|$ with $\theta_b = \alpha_m \cdot tanh[\beta_m \cdot (H - \beta_c)] + \alpha_c$. Here, H is the undisturbed bottom depth, $\eta(t)$ is the water elevation as a function of time. For the present application, the constant set employed is, $h_C = 2$, $\theta_s = 2$, $\alpha_m = 4.5$, $\alpha_c = 5.5$, $\beta_m = 0.1$ and $\beta_c = 20.0$. The parameter, β_c therefore is a switching depth to discriminate between the shallower and the deeper regions mentioned above. The nature of this σ-grid formulation is exemplified for three different depth regimes (shallow, moderate and deep say for a Bay or Estuary) in Figure 5.

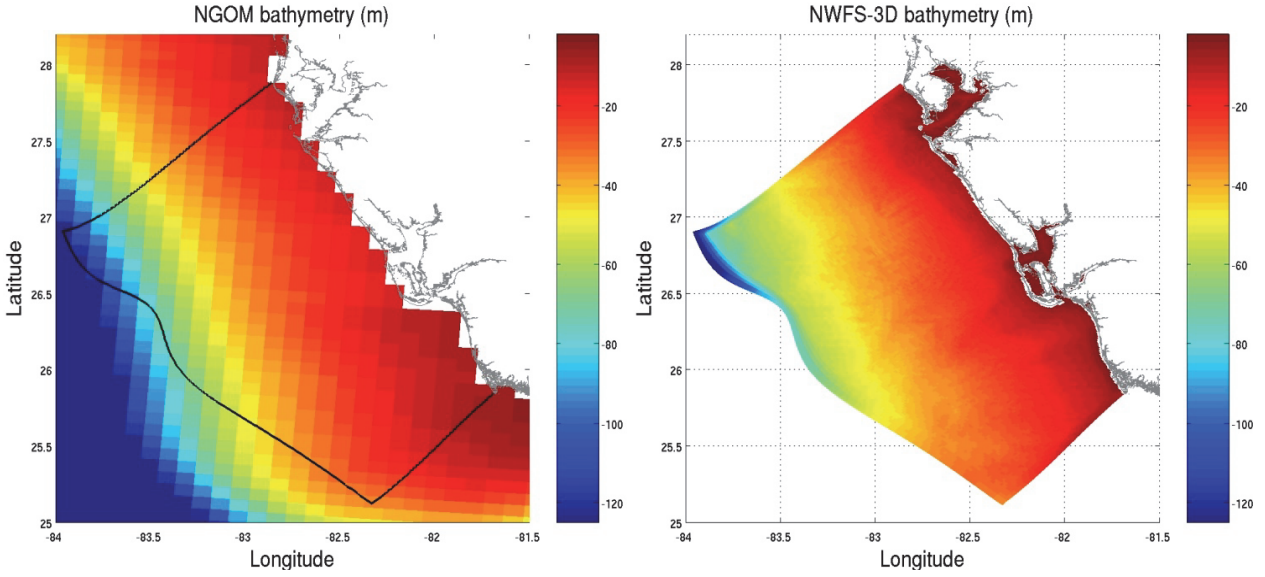

Figure 4. NGOM (left) and NWFS-3D (right) model bathymetries (m).

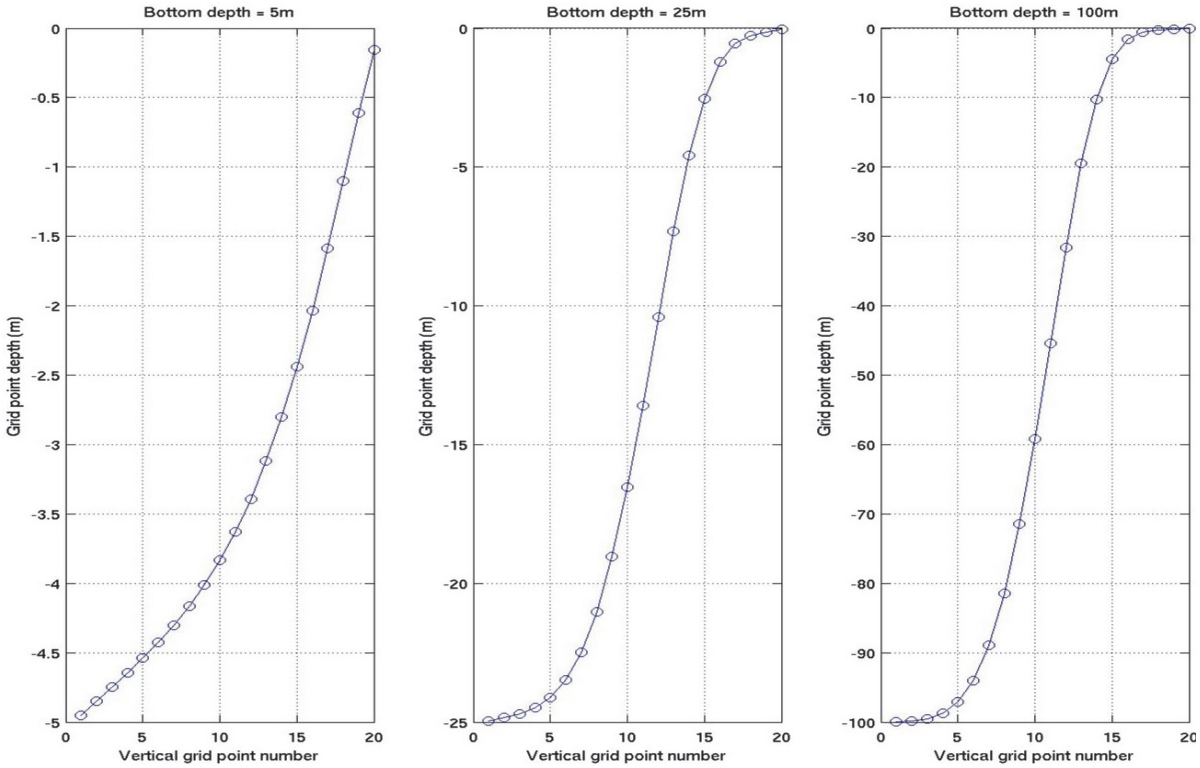

Figure 5. Vertical σ-grid point distribution for three bottom depth regimes.

3. COUPLING METHODOLOGY, INITIAL, BOUNDARY AND COMPATIBILITY CONDITIONS

The coupling methodology and the necessary conditions to achieve a valid and reliable coupling are described below.

3.1. Initial Conditions

The NWFS-3D model is spun-up from rest and the ensuing flow develops in response to the water elevation, temperature and salinity initialization fields. The NWFS-3D water elevation initialization field is derived via bilinear interpolation from the NGOM domain and the temperature and salinity fields are created through a tri-linear interpolation process. Numerical experiments where the model was initialized using also the currents fields from NGOM exhibited a high degree of numerical instability which is not unexpected. When the NWFS-3D model initialization time does not correspond exactly to a time value in the archived NGOM fields, the NGOM fields are first linearly interpolated in time before performing the spatial interpolations between the two model domains.

3.2. Surface and Bottom Boundary Conditions

The basin-scale NGOM model is forced at the surface using wind stresses and the barometric pressure produced by the U. S. Navy's Coupled Ocean/Atmosphere Mesoscale Prediction System (COAMPS). The pressure forcing is carried out using the inverted barometric effect method. COAMPS was developed by the Marine Meteorology Division (MMD) of the Naval Research Laboratory (NRL). The atmospheric components of COAMPS are used operationally by the U.S. Navy for short-term numerical weather prediction for various regions around the world. NGOM is also forced with monthly climatological net heat fluxes and Sea Surface Temperatures (SST) (developed by Dynalysis of Princeton, Princeton, NJ) the latter of which is needed to prevent NGOM SST drift in time. The wind stresses and barometric pressure are available hourly and the heat fluxes and SSTs are monthly climatologies. The SST forcing is carried out via a surface nudging mechanism (see below). At the ocean bottom, NGOM employs a quadratic bottom drag formulation with a drag coefficient, C_D of 0.0025 and for the heat fluxes, an insulating (zero flux) boundary condition is applied. Both at the surface and bottom, insulating conditions are employed for the salinity. Precipitation effects are not included.

In the coupled NWFS-3D set-up, the surface forcing is carried out by directly imposing the bilinearly interpolated NGOM wind stresses and net heat fluxes; barometric pressure forcing is brought in using the inverted barometric formulation applied to the bilinear interpolated NGOM pressure fields. The NGOM SST values are similarly interpolated on to the NWFS-3D domain and are nudged to through a nudging coefficient; this coefficient, α is estimated on the assumption that shortwave radiation flux incident upon the ocean surface penetrates to and is thus absorbed by 1.5 m (=Δz) of water over a duration of 1 day ($T_{day} = 86400$ seconds). This is also the formulation used in the NGOM model set-up. Hence, $\alpha = \rho C_p \Delta z / T_{day}$ where ρ, C_p are the sea water density and the specific heat capacity at constant pressure respectively. This nudging coefficient is constant in space. There are other spatially varying coefficient

formulations in the literature (for example, Young-Molling et al., 1997) which are relatively more sophisticated but they can be less straightforward to estimate.

The SST nudging in ROMS takes the form

$$H_s = H_s + \alpha \cdot (T_s - SST)$$

where H_s is the surface net heat flux, T_s is the model computed surface temperature and, SST is the NGOM interpolated (climatological) SST.

The bottom boundary conditions in the NWFS-3D model are the same as those in NGOM with also the same value for C_D. Again, as in NGOM, at the model surface and the bottom, an insulating boundary condition is employed for salinity and precipitation is not included.

3.3. Lateral Boundary Conditions

The NWFS-3D model is forced at the lateral open boundaries with water elevations, currents (both barotropic and baroclinic), temperature and salinity variables which have been spatially interpolated from the NGOM model output fields. These variables are brought in to the NWFS-3D model via the various open boundary condition options available within the ROMS model.

For model coupling the most obvious lateral boundary conditions to use would be the clamped conditions. These conditions would ensure all of the boundary data on the NWFS-3D domain would be identical to that of the NGOM domain at the corresponding spatial locations. However, such boundary conditions are known to be excessively restrictive whereby (i) barotropic waves are unable to enter and exit the NWFS-3D domain causing them to get trapped and possibly amplifying and (ii) the use of different vertical σ-grid formulations in the two model domains would cause a mismatch in the discrete, depth-averaged, barotropic velocities between them resulting in errorneous volume/mass transport in and out of the NWFS-3D domain. In order to address (ii), it was decided to re-compute the barotropic velocities on the NWFS-3D domain from the baroclinic velocities interpolated from the NGOM domain. To satisfy the first statement, (i), a numerical experiment was performed to investigate the propagation of barotropic waves within the NWFS-3D domain with the intention of discovering an ideal set of coupling boundary conditions.

The model set-up for the numerical experiment consisted of replacing the NWFS-3D bathymetry and coastline with those from NGOM model, generating (a) a set of initial conditions as explain in Section 3.1, (b) surface and bottom forcing fields as explained in Section 3.2 and (c) lateral boundary forcing variables by interpolating them from the NGOM domain on to the NWFS-3D boundary grid points. Thereafter, a pulse in the water elevation was introduced in (a) and the model was run to see how this pulse would propagate within NWFS-3D domain and also beyond it. The results are shown in Figure 6. Figure 6 (a) shows the initial condition where the pulse, located on the WFS is 16 cm higher than the surrounding water elevation level. It was found that using a higher pulse amplitude leads to model blow-up and a smaller amplitude did not show the reflected barotropic waves with sufficient clarity. The evolution of this pulse prior to impinging upon the model boundaries (both open ocean and land boundaries) is shown in Figure

6 (b). Further time evolution of the water elevation pulse, with the use of purely clamped boundary conditions, after impinging upon the model boundaries is shown in Figure 6 (c); it shows the reflected waves off the land and open ocean boundaries and they (roughly) have an amplitude half of the original pulse amplitude. Finally, in Figure 6 (d), where the elapsed time is the same as that for Figure 6 (c), the propagated pulse with the boundary conditions tabulated in Table 1 is shown. The wave pulse in Figure 6 (d) is quite similar to that in Figure 6 (c) in terms of the wave reflections from the land boundaries but it does not contain wave reflections from the open boundaries nor the wave "hot spots" at the open boundaries. Hence, in Figure 6 (d), the barotropic waves have been freely transmitted out through the open boundaries without them getting trapped within the computational domain which is unphysical.

In the boundary condition set given in Table 1, it is the use of the Flather conditions for the normal components of the barotropic velocity which renders the momentum boundary conditions non-reflecting. These boundary conditions have been employed by other investigators too (for example, see Korres and Lascaratos, 2003). Although Korres and Lascaratos use clamped conditions for temperature and salinity, in the present research, it was decided to use radiation conditions when there is outflow at lateral boundaries thereby allowing the tracers to evolve more naturally in time and space.

Flow variable name	**Optimal lateral boundary condition**
Water elevation	Clamped
Baroclinic velocities	Clamped
Tangential barotropic velocity	Clamped
Normal barotropic velocity	Flather
Temperature/Salinity	*Inflow* – Clamped and *Outflow* - Radiation

Table 1 : Optimal non-reflection open ocean coupling boundary conditions.

3.4. Other Coupling Compatibility Conditions

In addition to the above forcings, the NGOM model is also forced with rivers to include their volume discharges, water temperatures and salinities. Frequently, river salinity is assumed to be zero. In the coupled system, when there is overlap between the two model domains, the rivers from NGOM are included in the NWFS-3D model using the same river volume discharges, temperatures and salinities but at refined grid point locations (which are physically closest to the NGOM grid point locations). When however there is no overlap between the two domains – as in the Tampa Bay and Charlotte Harbor regions, additional rivers, if they exist, are included in the NWFS-3D model where their locations on the model grid match their actual geographical locations and their volume discharges, temperatures and salinities are prescribed from observed data which usually is from the US Geological Service (USGS). If the rivers are specified on the model grid at locations where tides are pronounced then, they are assumed to be tidal rivers and appropriate algorithmic changes have been made to the ROMS code to facilitate their effects.

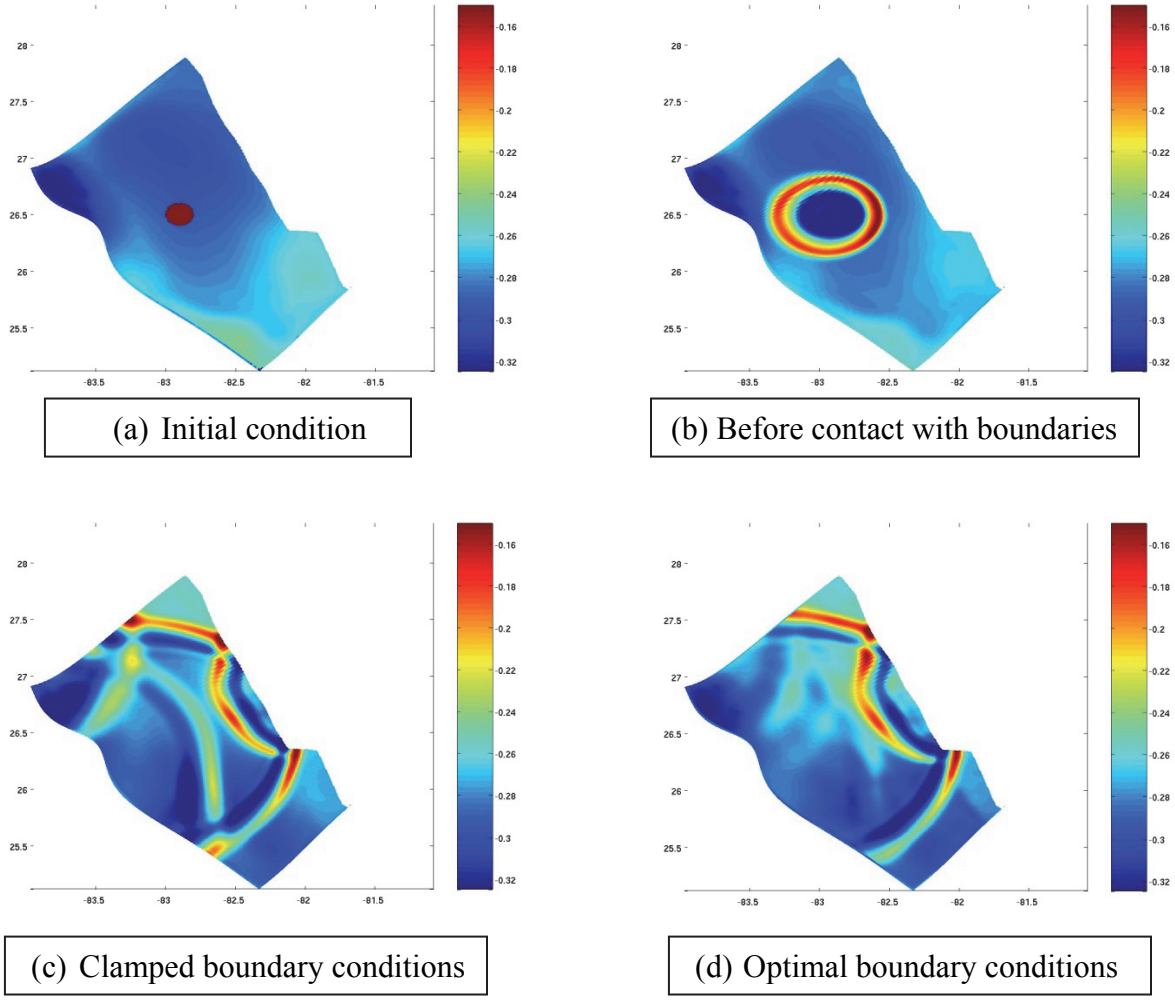

Figure 6. Water elevation (m) time evolution : propagation of a pulse in the NWFS-3D domain and the effect of lateral boundary conditions.

As explained in Section 2.0, it is necessary to reconcile the NWFS-3D bathymetry along the open ocean lateral boundaries with that of NGOM in order to ensure that the volume transport into NWFS-3D matches that exiting NGOM (that is, volume conservation). Therefore, even though the NWFS-3D model may have a higher resolution bathymetry which is more accurate than that of NGOM, the outer coupling model (NGOM) dictates the resolution and accuracy of the near-lateral-boundary bathymetry.

If the coupling system is driven purely with barotropic currents and water elevations then it is possible to maintain the correct transport between the two domains by scaling the normal barotropic velocity components by the bathymetric depth ratios at the lateral boundary grid points in the nested domain. However, when baroclinic velocities, temperature and salinity are involved too, this method fails to maintain : (i) the correct balance between the barotropic and baroclinic velocities and (ii) the heat and salt conservation between the two coupled model domains.

Finally, it is possible to implement the NGOM-NWFS-3D coupling in two ways : with or without volume conservation within the NWFS-3D domain. Some investigators, for example, Korres and Lascaratos, (2003) have chosen the former. Numerical experiments were conducted to test both options and it was discovered that during hurricanes and extreme meteorological phenomena, the conservation of volume led to a dampened response in the water elevations whereby the simulated elevations were not as high as prescribed by observations. The NWFS-3D water elevation predictions without the volume conservation constraint matched observations significantly more closely. As the WFS region is known to experience hurricanes regularly, it was decided not to force volume conservation within the NWFS-3D model.

4. COUPLING VALIDATION

The validity of the NGOM-NWFS-3D coupling was tested by running the NWFS-3D domain with the initial, boundary and compatibility conditions as stated in Sections 3.1 – 3.4 for the time period spanning June 15, 2005 to June 30, 2005. Therefore, the NGOM model was run first for this time period and thereafter, its model output fields were employed to generate the model initialization and forcing fields necessary for the NWFS-3D simulation. To make the two systems entirely compatible, (i) the NGOM bathymetry was also used for the NWFS-3D domain not only along the open boundaries but also throughout the domain and (ii) the NWFS-3D coastline was modified to emulate that of NGOM (thus deleting Tampa Bay and Charlotte Harbor). For (i), the NGOM bathymetry was interpolated on to the NWFS-3D domain via bilinear interpolation.

For the NWFS-3D ROMS model configuration, the Mellor-Yamada 2.5 vertical eddy-viscosity scheme was employed and the advection terms associated with the momentum and tracer equations were discretized using the third-order, upstream-biased discretization option. The latter option alleviated the need for using explicit numerical viscosity in the horizontal to remove spatial oscillations in the model solution fields. The baroclinic time step used was 240 seconds and the corresponding barotropic time step was 12 seconds. The adjustment process of the NWFS-3D model which was spun-up from rest was seen to occur over a period of approximately 7 simulation days.

The results of the 15-day model simulation are given in Appendix A. The (thin) black line in the plots associated with the NGOM fields is the open ocean boundary perimeter of the NWFS-3D domain. Figure A1 shows a comparison of the barotropic flow variables (water elevations, true east barotropic current and true north barotropic current) of NWFS-3D with those of NGOM. The comparison is seen to be close, in particular, for the currents. As expected, due to the finer model grid resolution, the NWFS-3D fields are seen to include small-scale details not contained in the NGOM fields. A comparison of the true eastern and true northern currents at a depth of 5m (approximate nominal ship draft depth) is given in Figure A2. Here too the comparison between the fields of NWFS-3D and those of NGOM is close and the currents fields of the former reflect the characteristics of the latter but with greater fine-scale detail. Finally, the potential temperature and salinity comparisons at a depth of 5m are shown in Figure A3 and the fields of NWFS-3D reflect the characteristics of those of NGOM whilst also including fine-scale details. Comparisons of currents, temperatures and salinities between the two models at other depths show a similar degree of agreement as well.

Therefore, these coupling initial, boundary and compatibility conditions have yielded a robust (numerically stable), accurate and reliable mechanism to couple the NWFS-3D model to the NGOM model. The fields of the former show the characteristics of the latter but with a greater content of small-scale detail as expected.

5. COUPLING APPLICATION TO A SYNOPTIC HINDCAST SIMULATION

This section describes the application of the NGOM-NWFS-3D coupled system to perform a realistic 6-month synoptic, hindcast simulation from June 15, 2005 to December 15, 2005 and the evaluation of the model outputs. The NGOM model was again run first for this time period and thereafter, its model output fields were employed to generate the model initialization and forcing fields necessary for the NWFS-3D simulation. The simulation period was chosen due to (a) the availability of NGOM model fields to provide initialization and forcing data for NWFS-3D, (b) the availability of observations to evaluate the output solution fields of NWFS-3D and NGOM and, (c) the occurrence of five hurricanes (Dennis, Emily, Katrina, Rita and Wilma) in the Gulf of Mexico which will severely test the robustness, reliability and accuracy of the coupled set-up. In this NWFS-3D configuration, the high resolution NOS sounding bathymetry and the NGDC medium resolution coastline are employed as described in Section 2.0 and it includes both Tampa Bay and Charlotte Harbor. Along the lateral open boundaries, the bathymetry has been matched with that of NGOM as also explained in Section 2.0.

The ROMS model configuration was identical to that for the coupling validation experiments in Section 4.0 but with the exception that, due to the long duration of the hindcast simulation (6-months), the ROMS perfect restart mechanism was employed and the simulation was continued in 1-month segments. The model was run on an IBM RS1000 platform using MPI parallelization with 96 processors. A single day of simulation consumed 2.53 minutes of wall clock time thereby giving a computational efficiency ratio of 1:568 which is highly efficient. Due to the fine grid resolution within the Tampa Bay and Charlotte Harbor regions, the baroclinic time step needed to be reduced to 90 seconds in order to maintain numerical stability which was ensured by monitoring the Courant-Lewy-Friedrichs (CFL) parameter.

In the generation of the NWFS-3D model initialization and surface forcing fields (wind stress, net heat flux, barometric pressure and SST fields), for the non-overlapping near shore, Tampa Bay and Charlotte Harbor regions (not present in the NGOM domain), a Nearest-Neighbor (NN) interpolation technique was employed. This interpolation method therefore, extended the NGOM model fields into these non-overlapping areas. For the initialization temperature and salinity fields, the interpolation was carried out along constant geopotential surfaces.

In the coupling validation exercise described in Section 4.0, the river forcing (volume transport, temperature and salinity) employed in the NWFS-3D model was identical to that of the NGOM model which involved only the Peace River. However, in the present application, due to the inclusion of Tampa Bay and Charlotte Harbor, a total of nineteen rivers are included in order to simulate the WFS temperature and salinity more realistically. The geographical locations of the river volume transport (blue circles) and river temperature/salinity (red triangles) data sources are shown in Figure 7 all of which are from the USGS; the river discharge locations themselves within the NWFS-3D model domain are shown as heavy black dots. Due to the relative sparsity of the temperature/salinity data sources, several rivers share the same temperature/salinity values. If multiple volume transport sources are available for each of the tributaries, their transports are combined together when generating the river forcing fields.

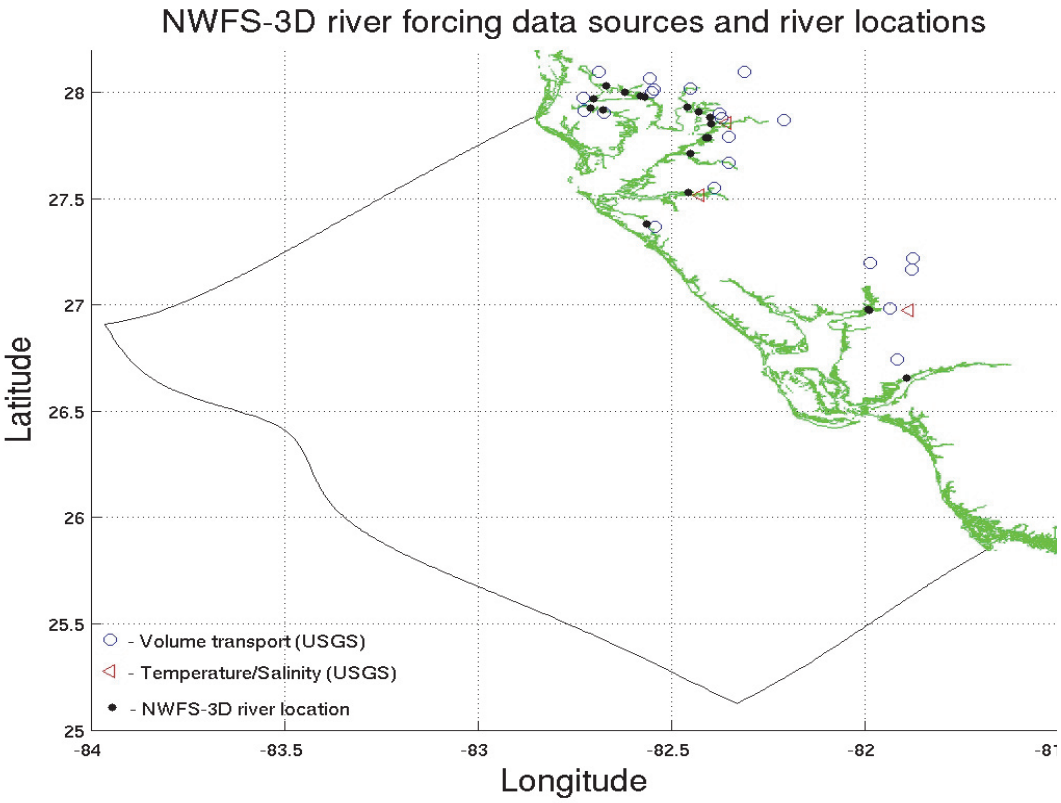

Figure 7. USGS river data source and river discharge locations in the NWFS-3D model.

5.1. Coupling Calibration Experiments

Numerical calibration experiments were performed in order to discover the optimal configurations for the meteorological forcing (possible further improvements to that described in Section 3.2), the vertical eddy-viscosity parameterization and the inclusion of tidal effects. These experiments are described below.

5.1.1. Calibration of the Surface Forcing

It was attempted to blend the COAMPS wind stresses, barometric pressure and the climatological net heat fluxes with values computed over the WFS from possible observational data sources. Such a blending would yield physically more realistic wind stress, barometric pressure and heat flux fields possibly also at a higher temporal frequency. An exhaustive search of observations yielded little usable data and they were sparsely spread in space and contained large gaps in their time-series. Hence, the forcing fields mentioned in Section 3.2 were employed.

5.1.2. Calibration of the Vertical Eddy-Viscosity Parameterization

Numerical calibration experiments in the Chesapeake Bay using ROMS showed that the vertical temperature and salinity stratification was quite sensitive to the vertical eddy-viscosity scheme employed (Lanerolle et al., 2011). The effect of the closure scheme on the water elevations and currents was minimal. The GLS k-ω scheme produced the best temperature and salinity values and stratification relative to observed data.

Similar experiments to examine the influence of the ROMS eddy-viscosity schemes on the temperature and salinity vertical stratification associated with the NWFS-3D model were performed. As before, the effect of the closure scheme on the water elevations and currents was negligible. Two 6-month synoptic hindcasts were run one with the Mellor-Yamda 2.5 scheme and the other with the GLS k-ω scheme. The vertical temperature and salinity profiles at 30 stations on the WFS were compared with each other and with observed data. These stations are plotted in Figure 8.

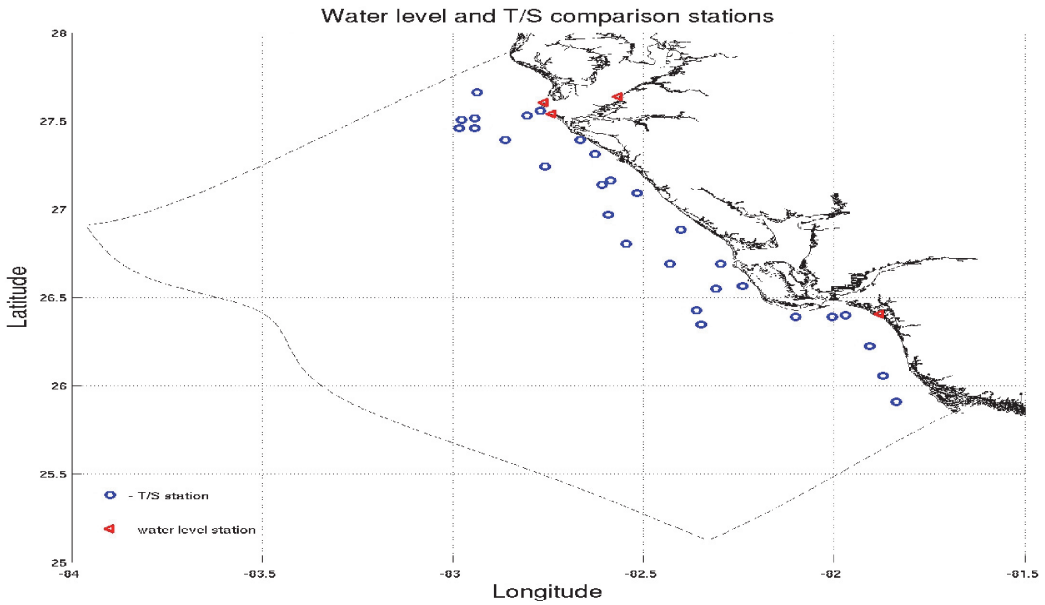

Figure 8. NWFS-3D model temperature and salinity comparison stations on the WFS.

Unlike in the Chesapeake Bay numerical experiments (Lanerolle et al., 2011), here, the model solutions were seen to be much less sensitive to the choice of eddy-viscosity closure scheme employed. Therefore, it was decided to adopt the Mellor-Yamada 2.5 scheme which also is computationally less expensive.

5.1.3. Calibration of the Tides

The NGOM model and hence also the NWFS-3D model inherently do not contain tides. It was therefore decided to investigate whether or not tides should be included in the latter to generate physically more realistic simulations for the WFS.

An ADvanced CIRCulation Model (ADCIRC, (Luettich et. al., [1992])) generated tidal harmonic constituent database has been created at NOAA/NOS/Office of Coast Survey (OCS)/ Coast Survey Development Laboratory (CSDL) (Feyen, 2008) using the EC2001 grid (EC2001, 2009). It contains the 37 standard NOS harmonic constituents (Tides & Currents, 2009) for water elevations and barotropic velocities (east and north components). These tidal constituents were bilinearly interpolated on to the NWFS-3D open boundary grid nodes and thereafter, predicted water elevation and barotropic velocity time-series were generated for the synoptic hindcast simulation time period (at each boundary node). Finally, these tidal time-series were added to their non-tidal counterparts generated previously (from the NGOM model fields as explained in Section 3.3) to get the full water elevation and barotropic velocity forcing fields at lateral boundaries.

Initial tidal simulations with the NWFS-3D model showed that the water elevations on the WFS were sufficiently accurate in terms of their phases but their amplitude comparisons with observations were somewhat poor. A comparison of the EC2001 and NWFS-3D model grid bathymetries along the NWFS-3D open boundaries showed that there were appreciable differences in value. Hence, the amplitudes of the interpolated harmonic constituents were scaled by the local bathymetric ratios to ensure that the tidal volume transport entering and exiting the NWFS-3D domain was consistent with that of ADCIRC. The resulting NWFS-3D model predicted water elevations showed a significant improvement in their agreement with observations. A comparison of water elevations at the entrance to Tampa Bay is shown in Figure 9. It can be inferred that the non-tidal NGOM and non-tidal NWFS-3D model water elevations are closely correlated with each other attesting to the validity of the coupling between the two models. The plot however also shows that it is the tidal-NWFS-3D model prediction which is able to follow the observed data and, the comparison between the two time-series is good both in terms of amplitude and phase. The non-tidal water elevations emulate a time-averaged counterpart of the tidal water elevations. Therefore, the inclusion of tides in the NWFS-3D model set-up is a necessity.

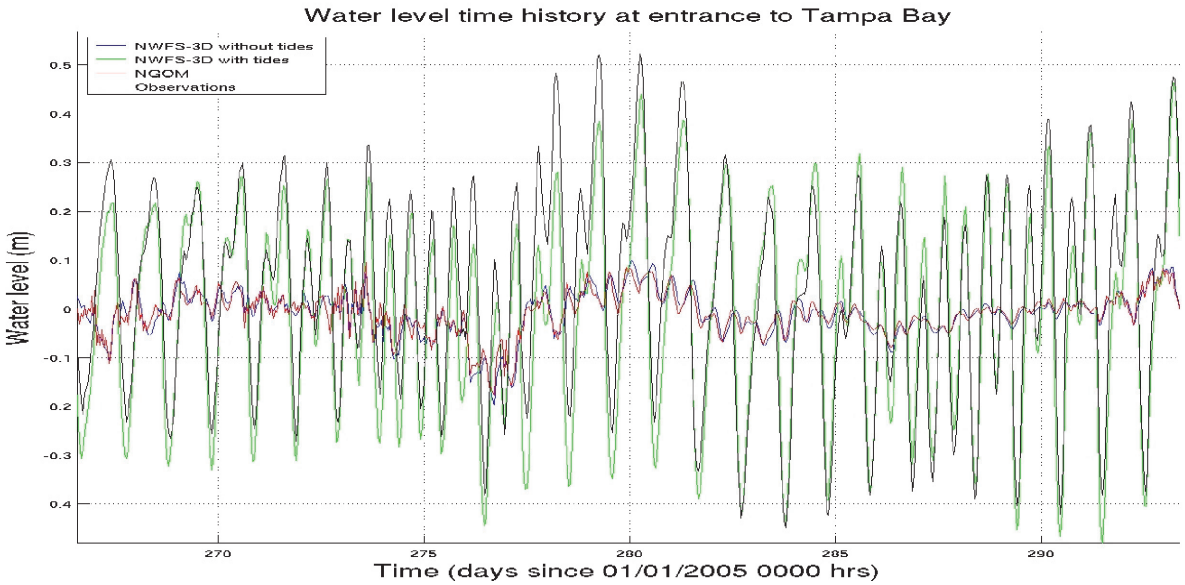

Figure 9. Water elevation comparison at the entrance to Tampa Bay with and without tides.

The model-observation comparison of the vertical temperature and salinity profiles conducted in Section 5.1.2 was now repeated by also including tides in the simulated results (still with the Mellor-Yamada 2.5 vertical eddy-viscosity scheme). It showed that the best overall comparisons were obtained by the model predicted profiles which contained tides. Hence, in addition to the water elevation comparisons, the temperature and salinity comparisons too clearly indicate the need for the inclusion of tides in the NWFS-3D model.

5.2. Comparison of Model Predictions with Observations

The NWFS-3D model results from the 6-month synoptic hindcast were evaluated against observations for water elevations, currents, temperature (T) and salinity (S) at the locations shown in Figure 10. The water elevation and currents data were from the University of South Florida's Coastal Ocean Monitoring and Prediction System (COMPS) (USF, 2010). The T and S data were from observations made by the Mote Marine Laboratory, Sarasota, FL (Mote, 2010).

5.2.1. Water Elevation Comparisons

The water elevation predictions from NWFS-3D and NGOM models are compared with observed data in Figure B1 (Appendix B) and some evaluation metrics are provided in Table 2. In these metrics, the raw Root Mean Square Error (RMSE) associated with the water elevations is split in to an amplitude and phase component following the method described in Lanerolle et. al, (2011) which is more pertinent for wave-like phenomena such as water elevation time-series. Comparison stations WL1 and WL4 (Figures 10 and B1) were selected as the former is representative of the three stations in the vicinity of Tampa Bay and the latter is the only other station available for comparison and is in a different region of the model domain. The water elevation time-histories in Figure B1 (panels 1 and 3) show that the NWFS-3D model predictions follow the observations closely specially at station WL1. The predictions at station WL4 clearly show amplitude errors and the model predominantly over-predicts the water elevations relative to observations. The predictions from NGOM are seen to be devoid of tides and they emulate a temporally averaged version of the NWFS-3D predictions as expected. Table 2 shows that water elevation model errors are small in and around Tampa Bay and they satisfy the NOAA/NOS water elevation skill assessment limit of being under 15 cm in amplitude and 15 minutes in phase (Zhang et. al, 2009). With regards to station WL4, both the amplitude and phase errors are bigger than those near Tampa Bay and this could be due to it being in a marshy area within an embayment which is not adequately resolved in the NWFS-3D model grid (and the sediment dominated dynamics not accounted for). The amplitude error at WL4 however is still within the acceptable NOAA/NOS skill assessment limit. To get a clearer understanding of the water elevation model predictions for extreme events (the hurricanes), they were filtered using a 39-hour low pass filter (Figure B1, panels 2 and 4) to de-tide them. They show that : (i) the NGOM and NWFS-3D model predictions are practically coincident thus attesting to the validity of the model coupling and (ii) the model predictions are able to discern the hurricane water elevations, although some amplitude and phase errors are apparent. The unfiltered water elevations (panels 1 and 3) also confirm (ii). The water elevation time-series also prove that both models are able to transition in to and recover from hurricanes correctly which is evidence that the NGOM-NWFS-3D coupled system is numerically stable, robust and reliable during both

when meteorological events are present and when they are not. The coupled system was not developed exclusively as a hurricane modeling system.

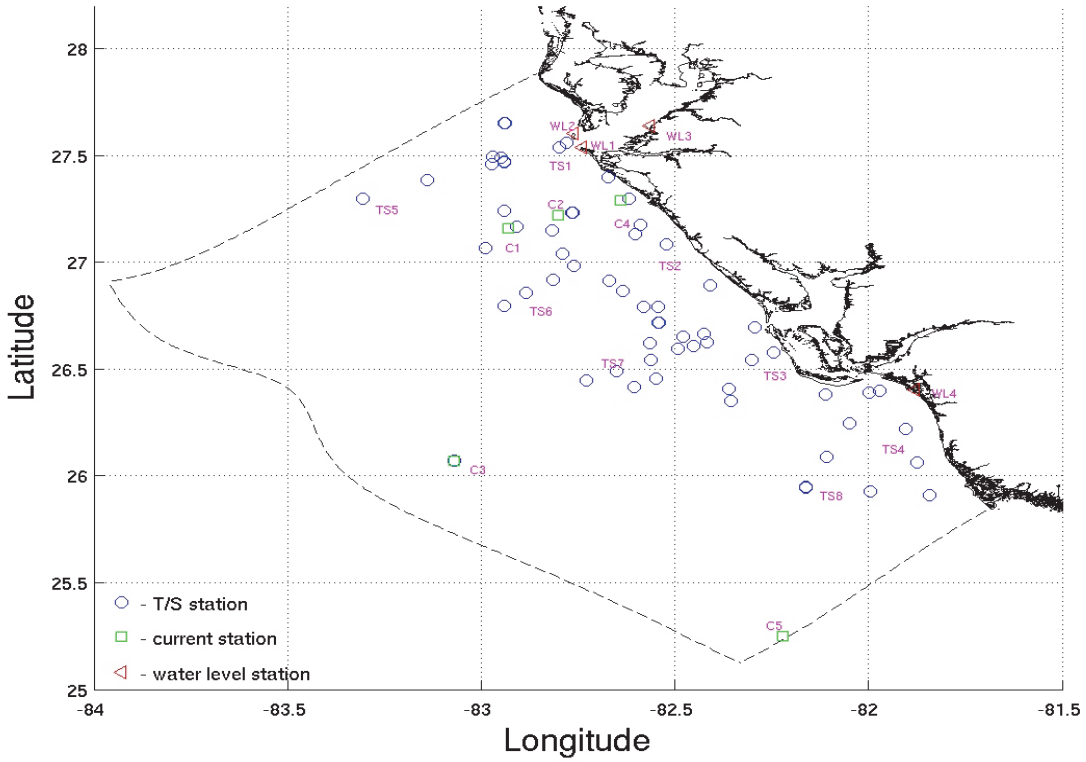

Figure 10. Water elevation (WL1-WL4), current (C1-C5) and T/S (TS1-TS8) model-observation comparison stations in the NWFS-3D model domain.

Station ID	Amplitude error (cm)	Phase error (hours)
WL1	9.9	-0.05
WL2	11.4	-0.08
WL3	10.4	-0.12
WL4	14.6	0.83

Table 2. Amplitude and phase errors for the water elevations at stations shown in Figure 10.

5.2.2. Currents Comparisons

The currents time-series for stations C2 and C4 (Figure 10) are plotted in Figure B2 (Appendix B) and some evaluation metrics are provided in Table 3. Stations C2 and C4 are University of South Florida's COMPS-ADCP/oldEC4 and COMPS-ADCP/old EC5 stations respectively. These two stations were selected because both their tidal and non-tidal components of the currents time-series are clearly discernable. For stations on or close to the shelf, the currents analyses were performed by rotating them to along-shore and cross-shore components but at

other stations, they were carried out in their true eastern and true northern directions. All of the currents plots and analyses were generated at a depth of 5m (nominal depth of ship's draft) and similar inferences and conclusions can be made for currents at other depths too.

The currents time-series plots in Figure B2 show that the along-shore component is significantly larger in magnitude than its cross-shore counterpart. However, it is the latter (panels 1 and 3) which contains most of the tidal signal and the NWFS-3D model predictions are able to follow the observations closely and the main error contribution is from amplitude mismatches. As expected, the NGOM model predictions are a time-averaged version of those from the NWFS-3D model due to the lack of tides. The along-shore currents components (panels 2 and 4) show that the NWFS-3D model predictions have a weak tidal signal and are not appreciably different to those from the NGOM model and they both in general follow the observations. The observed time-series however include a relatively stronger tidal signal. The model predictions account for the hurricanes but during them, the currents amplitudes are somewhat over-predicted.

Stn. ID	Current Analysis Orientation	U-current		V-current	
		Amp. Err (cm/s)	Phs. Err (hrs.)	Amp. Err (cm/s)	Phs. Err (hrs.)
C1	Cross-Along Sh.	4.4	-0.15	6.2	0.07
C2	Cross-Along Sh.	2.8	-0.05	5.2	-2.07
C3	True East-North	5.9	0.85	5.3	-0.37
C4	Cross-Along Sh.	2.7	0.05	5.4	-0.25
C5	True East-North	8.9	0.72	8.3	-0.67

Table 3. Amplitude and phase errors for currents at comparison stations shown in Figure 10. Depending on the current analysis orientation, the U-current is either in the true east or cross-shore direction and the V-current is either in the true north or along-shore direction.

The error metrics given in Table 3 are for currents which have been de-meaned and filtered via a 39-hour low-pass time filter so as to expose the tidal signals associated with the along-shore current component better. The de-meaning was carried out for both model generated currents time-series and also observations. They show that the current amplitude errors are well below 26 cm/s which is the NOAA/NOS current skill assessment limit (Zhang et. al, 2009). The main source of error therefore is in the phases and due to the presence of a relatively stronger tidal signal, the errors in the cross-shore currents are smaller than those in the along-shore currents. For the latter, at station C2, the amplitude-phase error splitting algorithm (Lanerolle et. al, 2011) fails and the resulting phase error is quite large. The algorithm is only valid for comparing two oscillatory time-series which are generally similar to each other and are composed of similar tidal harmonic constituents and where the tidal signal is discernable. For the stations beyond the shelf break (stations C3 and C5) the currents were analyzed in the true eastern and true northern directions. Although the amplitude errors are well within the acceptable range (0-26 cm/s), the phase errors are quite large.

5.2.3. Temperature and Salinity Comparisons

The T and S model-observation comparisons are given in Figures B3-B7 (Appendix B). Figures B3 and B4 show the vertical stratification comparisons at discrete dates for stations TS1-TS8 and Figures B5-B7 show the comparisons over time at 65 Mote measurement stations (on the WFS as shown in Figure 10) but at discrete vertical (geopotential) depths of 5m, 10m and 15m. Hence, the former provides a local picture and the latter provides a global picture or general assessment of the nature of T, S predictions from the NWFS-3D model.

In the vertical stratification comparisons in Figures B3 and B4, the T and S profiles predicted by NWFS-3D model are given at the exact times and also at an hour before and an hour after them so as to account for any errors associated with the tides. The vertical T and S profiles show that : (i) the sloshing motion of the tides has a negligible effect on the profiles, (ii) in general, the vertical stratification associated with the modeled results and the observations is weak and there is no seasonal dependence (also true for the other T/S comparison stations shown in Figure 10) over the 6-month simulation period, (iii) the observations show relatively stronger stratification than the model predictions (e.g. the salinity profile for station TS3), (iv) the NWFS-3D and NGOM model predicted profiles are close to each other and more so than to the observed profiles; for T, the model profiles are generally about 0.5 ^{o}C apart with neither model being consistently cooler or warmer than the other and for S, they are about 0.5 PSU apart with the NWFS-3D model predictions being fresher in general and, (v) neither model convincingly compares better with observations than the other; for T, they are 0.5^{o}C – 1.5^{o}C cooler than the observations and for S, model predictions are saltier by 0 PSU – 3 PSU at the near-shore stations (TS1-TS4) and are fresher than observations by 0.25 PSU – 1.0 PSU at stations beyond the shelf break (TS5-TS8).

The model-observation comparison of T at constants depths of 5m,10m and 15m given in Figures B5-B7 indicate that : (i) a seasonal cooling from July-December is clearly visible in the observations and the model predictions, (ii) a cooling behavior is also seen when moving deeper down the water column from 5m to 10m and from 10m to 15m, (iii) the general model-observation comparisons at 5m, 10m and 15m depths are similar, which is consistent with the weak vertical stratification seen (Figures B3-B4), (iv) in the warmer months of July-October, the model predictions are cooler than the observations with predictions of NGOM being cooler than those of NWFS-3D; in the cooler months – for example, December, the converse is true and the model predictions are warmer than observations with NGOM being the warmest. The difference between model predictions and observations is generally in the range of 1^{o}C – 2^{o}C and the excessive cooling/heating could be attributed to the use of the monthly climatological net heat fluxes in the meteorological forcing. This trend may be able to be eliminated or curtailed by using the ROMS Bulk Flux formulation with realistic meteorological forcing data (wind speeds, air pressure, air temperature, net shortwave radiation flux and downward longwave radiation flux). However, then, the meteorological forcing may become inconsistent with the tides-enhanced, open boundary forcing fields from the NGOM model (which is forced with COAMPS wind stresses, air pressure; climatological net heat fluxes) and the coupled system could become numerically unstable.

The S model-observation comparisons in Figures B5-B7 at 5m, 10m and 15m depths show that : (i) unlike for T, there is no obvious seasonal variation in S, (ii) the greatest spread in values of S between NWFS-3D and NGOM model predictions and also between the model predictions and observations is at the 5m depth and in the July-August time which is the warmest season, (iii) the average S value increases with depth as expected, (iv) at 5m, the spread in values of observed S is greater than those of the model predictions and the latter is excessively salty with NGOM model predictions being the saltiest; the general discrepancy between predictions and observations is about 2 PSU but upon approaching the winter season, the observations and predictions show convergence toward each other, (v) at the 10m depth, the spread in the S values is significantly less than that at 5m and the model-observation agreement is also better; during the fall-winter season, NWFS-3D model predictions are about 0.5 PSU fresher than those of NGOM which shows closer agreement with observations and (vi) at 15m, there is close agreement between the model predictions and observations with the exception in November, when the predictions are seen to be fresher than observations with the NWFS-3D model predictions being the freshest by about 1 PSU.

The NOAA/NOS skill assessment limits state that model predicted and observed T values should be within 2 ^{o}C of each other and the corresponding S differences should to be within 3.5 PSU (Zhang et. al, 2009). The above T and S validation exercises have shown that the NWFS-3D model predictions (and also those of the NGOM model) do satisfy these limits.

6. SUMMARY, CONCLUSIONS AND FUTURE DIRECTIONS

Global and basin-scale numerical ocean models run on model grids which are too coarse to resolve most bays, estuaries and embayments. Generating bay and estuary resolving grids for such models on the other hand would produce grids with prohibitively large numbers of grid points and the time step restrictions for running on such grids would also be unacceptably strict. Therefore, model coupling (or nesting as also commonly known) is a reasonable way to downscale global/basin-scale models to perform spatio-temporally high resolution computations in localized regions. Model coupling can be achieved via : two-way nesting within the same model or by coupling two separate models (sharing common interfaces) one of which could be a global/basin-scale model. Due to the greater degree of flexibility associated with the latter, it is preferred over the former and hence is also adopted in the present research.

In this report, the coupling of a ROMS-based model for the west Florida shelf to a larger, POM-based, basin-scale Gulf of Mexico model is described. The former, named NWFS-3D includes both Tampa Bay and Charlotte Harbor which were not contained in the latter which is called NGOM. The coupling is effected via the T and S initialization fields, lateral and surface boundary condition fields all of which are interpolated on to the NWFS-3D model grid from the NGOM grid using bi-linear or tri-linear interpolation techniques. The ideal lateral boundary condition set was to use clamped conditions for water elevations and baroclinic velocities, Flather-clamped conditions for the normal and tangential barotropic velocities (respectively) and a radiation-clamped condition for T and S depending on whether there was outflow or inflow at the boundary (respectively). It is this specific boundary condition set which enabled the NWFS-3D model to be able to transmit barotropic waves freely in and out of the model domain, while a purely clamped set of boundary conditions led to the trapping of these waves resulting in unphysical model solutions. Additionally, any NGOM domain river forcing was also consistently included in the NWFS-3D domain together with bathymetry matching along the open ocean boundaries to ensure consistency in the volume transport between the two domains. It was discovered that enforcing volume conservation within the NWFS-3D model resulted in a dampened response to extreme meteorological phenomena and therefore, this condition was not specified. A novel terrain-following σ-coordinate grid was employed in the vertical which resolved the bottom boundary layer in shallow regions and both the bottom and surface boundary layers in the deeper regions.

The model coupling was validated by performing a 15-day simulation using the low-resolution bathymetry and coastline from the NGOM model in the NWFS-3D model also. This model domain did not include Tampa Bay or Charlotte Harbor. A comparison of the water elevations, barotroic currents, baroclinic currents, T and S showed that the NWFS-3D model was able to faithfully reproduce the corresponding fields from the NGOM model.

The coupled system was then employed to perform a 6-month synoptic hindcast simulation from June 15, 2005 to December 15, 2005 for which NGOM fields and observed data were available. This period also included five hurricanes (Dennis, Emily, Katrina, Rita, Wilma) which enabled the numerical stability, robustness and reliability of the coupled system to be severely tested. Initial calibration exercises allowed the optimal surface forcing fields and vertical eddy-viscosity scheme to be isolated and they also showed a need for the inclusion of tides in the computations.

Furthermore, unlike in the NGOM model where only the Peace River was included, in the NWFS-3D model, nineteen rivers were included primarily due to the inclusion of Tampa Bay and Charlotte Harbor. Comparison of the NWFS-3D water elevations, currents, T and S with observations showed that they were in good general agreement with each other and within the NOAA/NOS skill assessment limits (within 15 cm for water elevation amplitudes, 26 cm/s for currents speeds, 2^{o}C for T and 3.5 PSU for S). For T and S, the NWFS-3D model predictions were consistent with those of the NGOM model and neither model showed a strong advantage over the other in its agreement with observed data.

Future research directions could involve : (i) re-running the synoptic hindcast simulation with a range of surface forcing meteorological products (for example, those from the NOAA/National Weather Service's (NWS's) Global Forecast System (GFS), the North American Regional Renalysis (NARR) model, the NWS National Digital Forecast Database (NDFD), etc.) to possibly further improve the NWFS-3D model predictions and obtain ensemble predictions and (ii) the operationalization of the NWFS-3D model set-up to run in real-time and generate daily model forecasts for the WFS region.

The coupling methodology designed and proven in this report are sufficiently general and flexible that they are not restricted to modeling applications in WFS region only but are generally applicable to any region around the world.

ACKNOWLEDGEMENTS

The authors wish the thank Dr. Frank Aikman III, Branch Chief of the CSDL's Marine Modeling and Analysis Programs (MMAP) for his management support. Professor Robert H. Weisberg of the College of Marine Science, University of South Florida (USF) is gratefully acknowledged for providing the water elevation and current observations for model validation. The Mote Marine Laboratory and Dr. Gary Kirkpatrick are also gratefully acknowledged for providing the temperature and salinity observations for model validation.

REFERENCES

Alvera, A., Barth, A., and Weisberg, H. R., 2009. A nested model of the Cariaco Basin (Venezuela): description of the basin's interior hydrography and interactions with the open ocean, *Ocean Dynamics,* 59, pp. 97-120.

Berliand, M. E. and Berliand, T. G., 1952. Determining the net longwave radiation of the earth with consideration of the effects of cloudiness (in Russian), *Izv. Akad. Nauk SSSR,* Ser. Geofiz 1.

Blayo, E. and Debreu, L., 2006. Nesting Ocean Models (Chapter 5), *Ocean Weather Forecasting : an integrated view of oceanography (Ed. Eric P. Chassignet, Jacques Verron, Springer)*, pp. 127-147.

Debreu, L. and Blayo, E., 2008. Two-way embedding algorithms : a review, *Ocean Dynamics,* 58, pp. 415-428.

EC2001, 2009. http://www.unc.edu/ims/ccats/tides/tides.htm

Fairall, C.W., E.F. Bradley, D.P. Rogers, J.B. Edson and G.S. Young, 1996a: Bulk parameterization of air-sea fluxes for tropical ocean-global atmosphere Coupled-Ocean Atmosphere Response Experiment, *Journal of Geophysical Research*, Vol. 101, pp. 3747-3764.

Fairall, C.W., E.F. Bradley, J.S. Godfrey, G.A. Wick, J.B. Edson, and G.S. Young, 1996b: Cool-skin and warm-layer effects on sea surface temperature, *Journal of Geophysical Research*, Vol. 101, pp. 1295-1308.

Feyen, J., 2008, Personal communication.

Korres, G., and Lascaratos, A., 2003. http://pelagos.oc.phys.uoa.gr/mfstep/ ALERMO_MFSTEP_DETAILS.htm

Kourafalou, V. H., and Tsiaras, K. P., 2007. A nested circulation model for the North Aegean Sea, *Ocean Sci.*, 3, 1-16.

Lanerolle, L. W. J., Patchen, R. P. and Aikman III, F., 2011. The second generation Chesapeake Bay Operational Forecast System (CBOFS2) : Model development and skill assessment, *NOAA Technical Report NOS CS* 29.

Liu, W. T., Katsaros, K. B. and, Businger, J. A., 1979. Bulk parameterization of the air-sea exchange of heat and water vapor including the molecular constraints a the interface, *Journal of Atmospheric Sciences*, Vol. 36, pp. 1722-1735.

Luettich, R.A., Westerink J. J., and Scheffner N. W., 1992. ADCIRC: an advanced three-dimensional circulation model for shelves coasts and estuaries, report 1: theory and methodology of ADCIRC-2DDI and ADCIRC-3DL, *Dredging Research Program Technical Report DRP-92-6*, U.S. Army Engineers Waterways Experiment Station, Vicksburg, MS, 137p.

Mellor, G. L., and Yamada, T., 1982. Development of a turbulence closure model for geophysical fluid problems, *Reviews of Geophysics and Space Physics*, Vol. 20, pp. 851-875.

Mote, 2010. Personal communication with Richard Patchen (NOAA/NOS/OCS/CSDL)

SeaGrid, 2009. http://woodshole.er.usgs.gov/operations/modeling/seagrid/seagrid.html

Shchepetkin, A. F. and McWilliams, J. C., 1998. Quasi-monotone advection schemes based on explicit locally adaptive dissipation, *Monthly Weather Review*, Vol. 126, pp. 1541-1580.

Shchepetkin, A. F. and McWilliams, J. C., 2003. A method for computing horizontal pressure-gradient forcing in an oceanic model with a nonaligned vertical coordinate, *Journal of Geophysical Research*, Vol. 108, No. C3, pp 1-34.

Shchepetkin, A. F. and McWilliams, J. C., 2004. The Regional Oceanic Modeling System : a split-explicit, free-surface, topography-following-coordinate ocean model, *Ocean Modelling*, Vol. 9 (4), pp. 347-404.

Sheng, J., Greatbatch, R. J., Zhai, X. and Tang, L., 2005. A new two-way nesting technique for ocean modeling based on the smoothed semi-prognostic method, *Ocean Dynamics*, 55, 162-177.

Song, Y. T., and Haidvogel, D. B., 1994. A semi-implicit ocean circulation model using a generalized topography following coordinate system, *Journal of Computational Physics*, Vol. 115, pp. 228-244.

Styles, R., and Glenn, S. M., 2000. Modeling stratified wave and current bottom boundary layers in the continental shelf, *Journal of Geophysical Research*, Vol. 105, pp. 24119-24139.

Tides & Currents, 2009, http://www.tidesandcurrents.noaa.gov /station_retrieve.shtml?type=Harmonic+Constituents

USF, 2010. Personal communication with Richard Patchen (NOAA/NOS/OCS/CSDL)

Warner, J. C., Sherwood, C. R., Arango, H. G., and Signell R. P., 2005. Performance of four turbulence closure methods implemented using a generic length scale method, *Ocean Modelling*, Vol. 8, pp. 81-113.

Weisberg, H. R., Barth, A., Alvera-Azcarate, A. and Zheng, L., 2009. A coordinated coastal ocean observing and modeling system for the West Florida Continental Shelf, *Harmful Algae*, 8, pp. 585-597.

Young-Molling, C., C., da Silva, A. M., and Levius, S., 1997. Atlas of surface marine data 1994 volume 6 : heat flux sensitivity to sea surface temperature, *NOAA Atlas NESDIS 12*, xii-xv.

Zavatarelli, M. and Pinardi, N., 2003. The Adriatic Sea modeling system : a nested approach, *Annales Geophysicae*, 21, 345-364.

Zhang, A., Hess, K., Wei, E. and Myers, E., 2009. Implementation of model skill assessment software for water elevation and current in tidal regions, *NOAA Technical Report*, NOS CS 24.

APPENDIX A. COUPLING VALIDATION

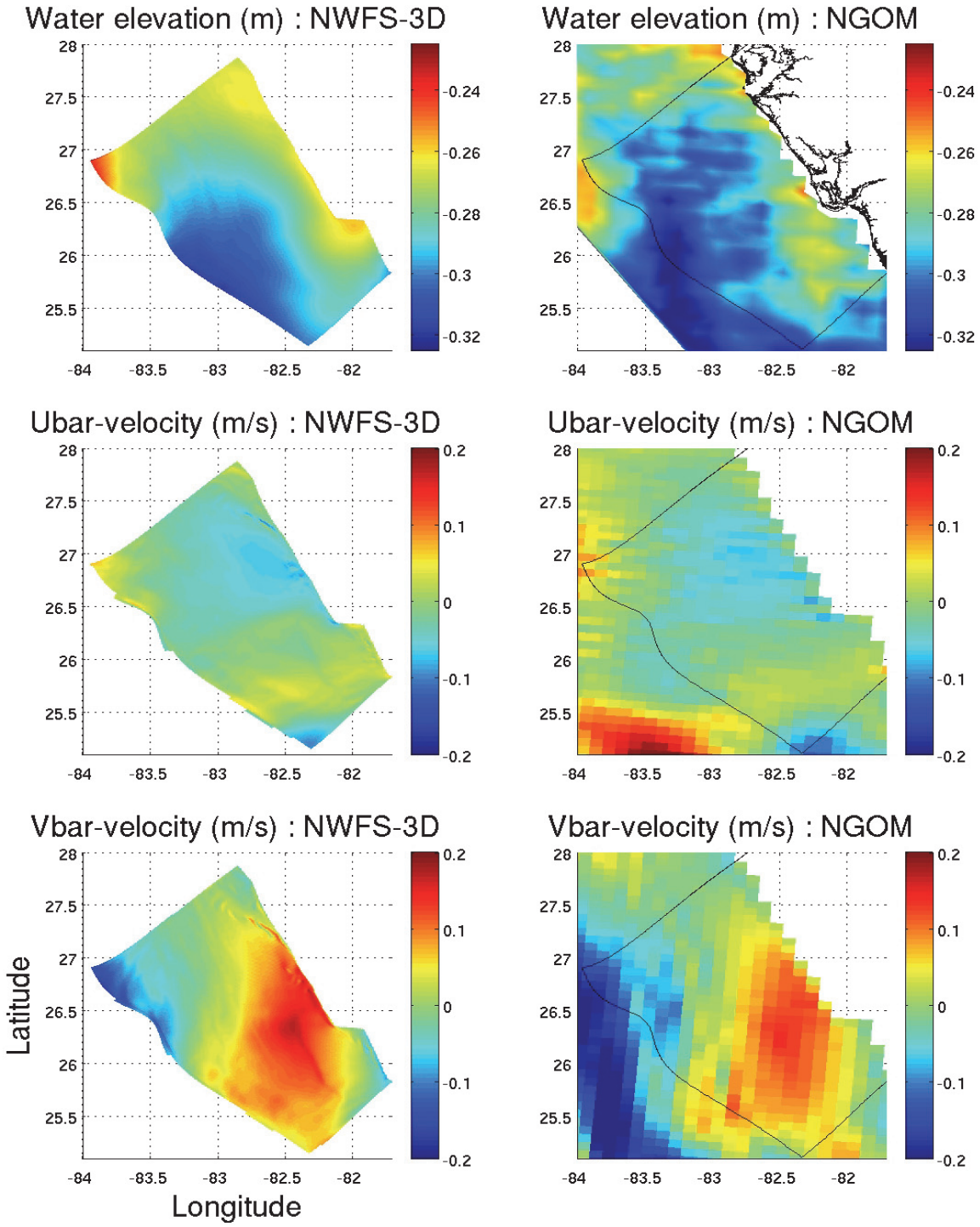

Figure A1. Comparison of the barotropic flow variables (water elevations and currents).

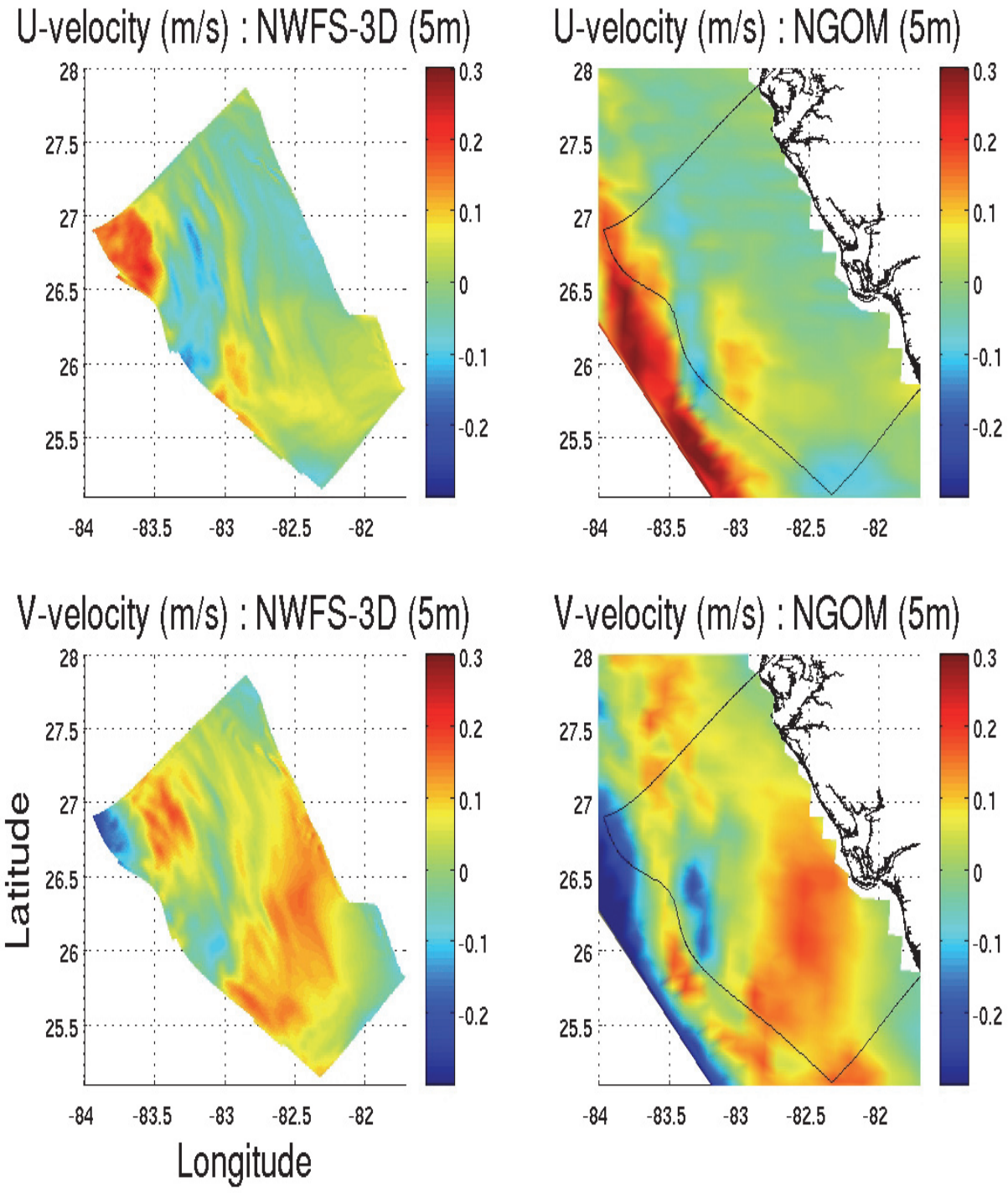

Figure A2. Comparison of the U- (true east) and V- (true north) currents components at a depth of 5m.

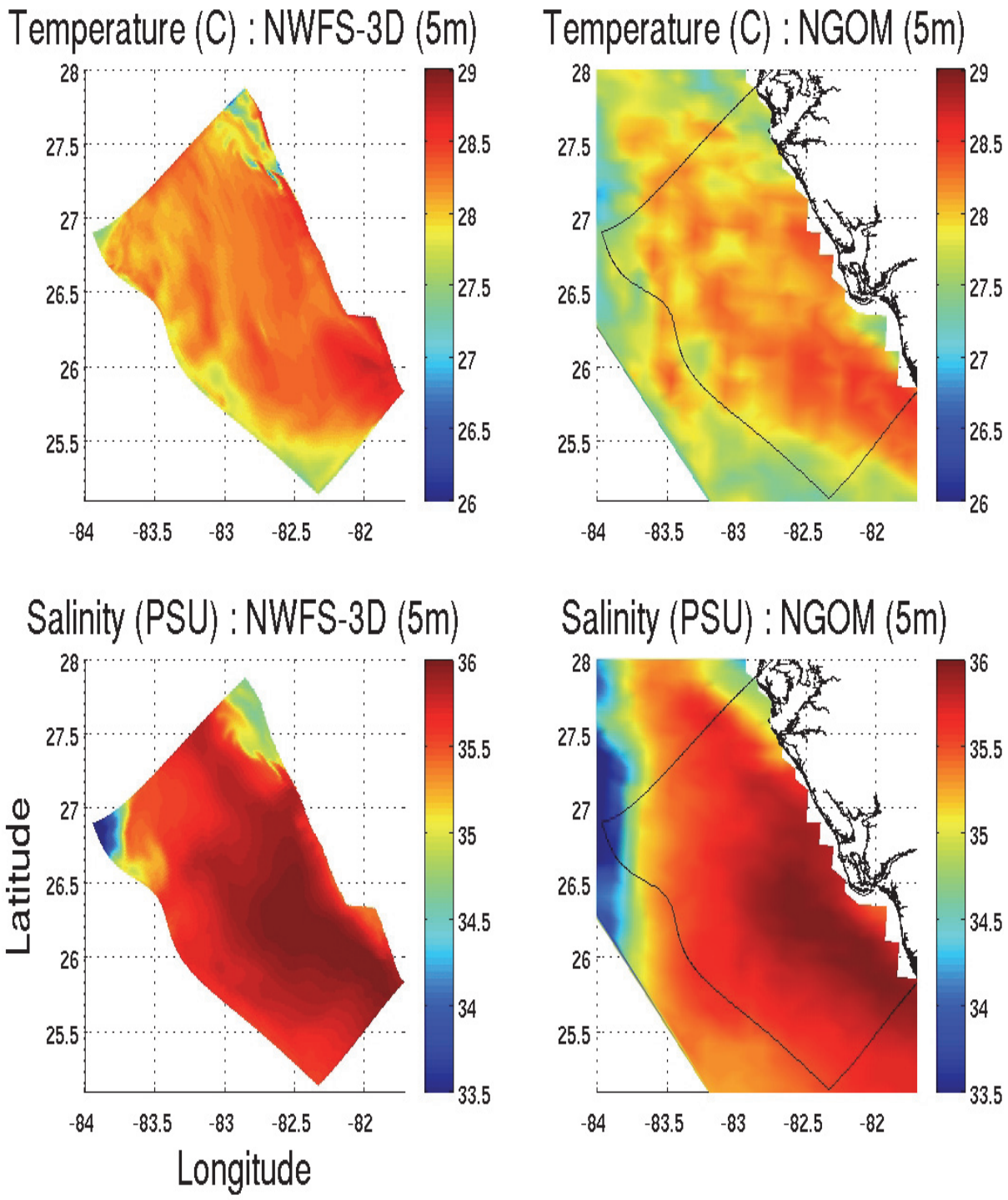

Figure A3. Comparison of the temperature and salinity at a depth of 5m.

APPENDIX B. COUPLING APPLICATION TO A SYNOPTIC HINDCAST SIMULATION

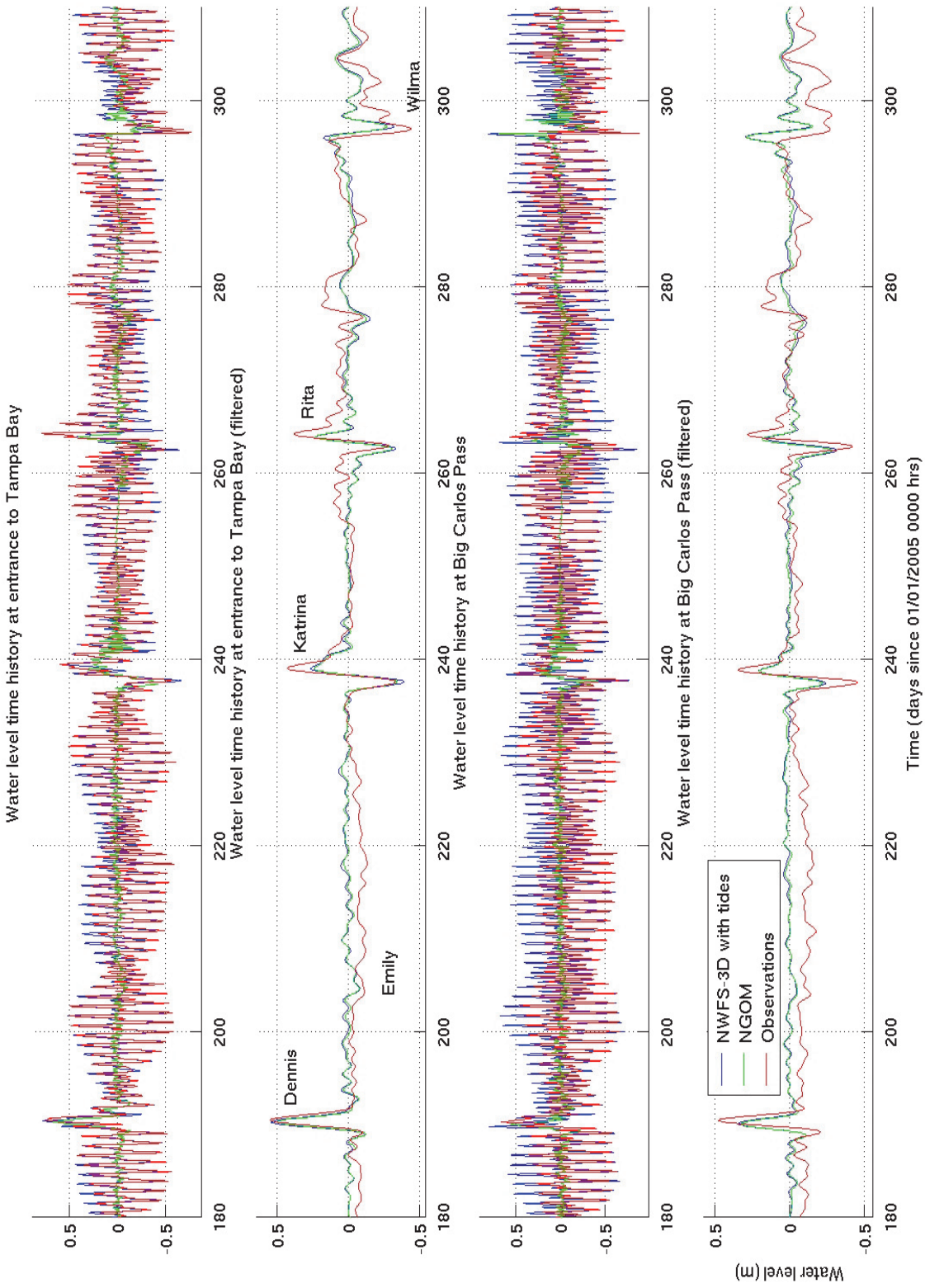

Figure B1. Water elevation model-observation comparisons at Tampa Bay (WL1) entrance and Big Carlos Pass (WL4).

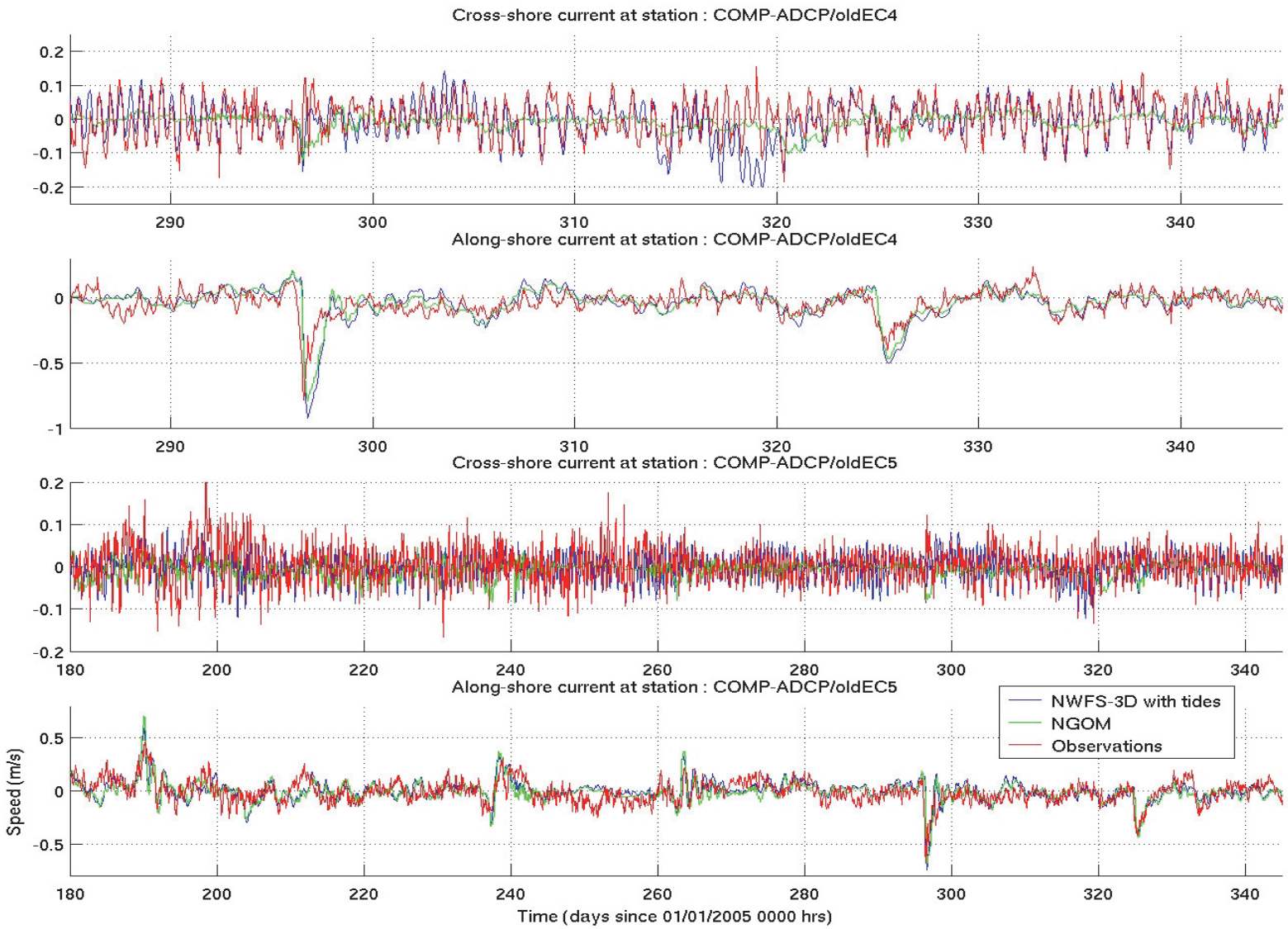

Figure B2. Model-observation comparison of the 5m depth currents at COMP-ADCP EC4 (C2) and EC5 (C4) stations.

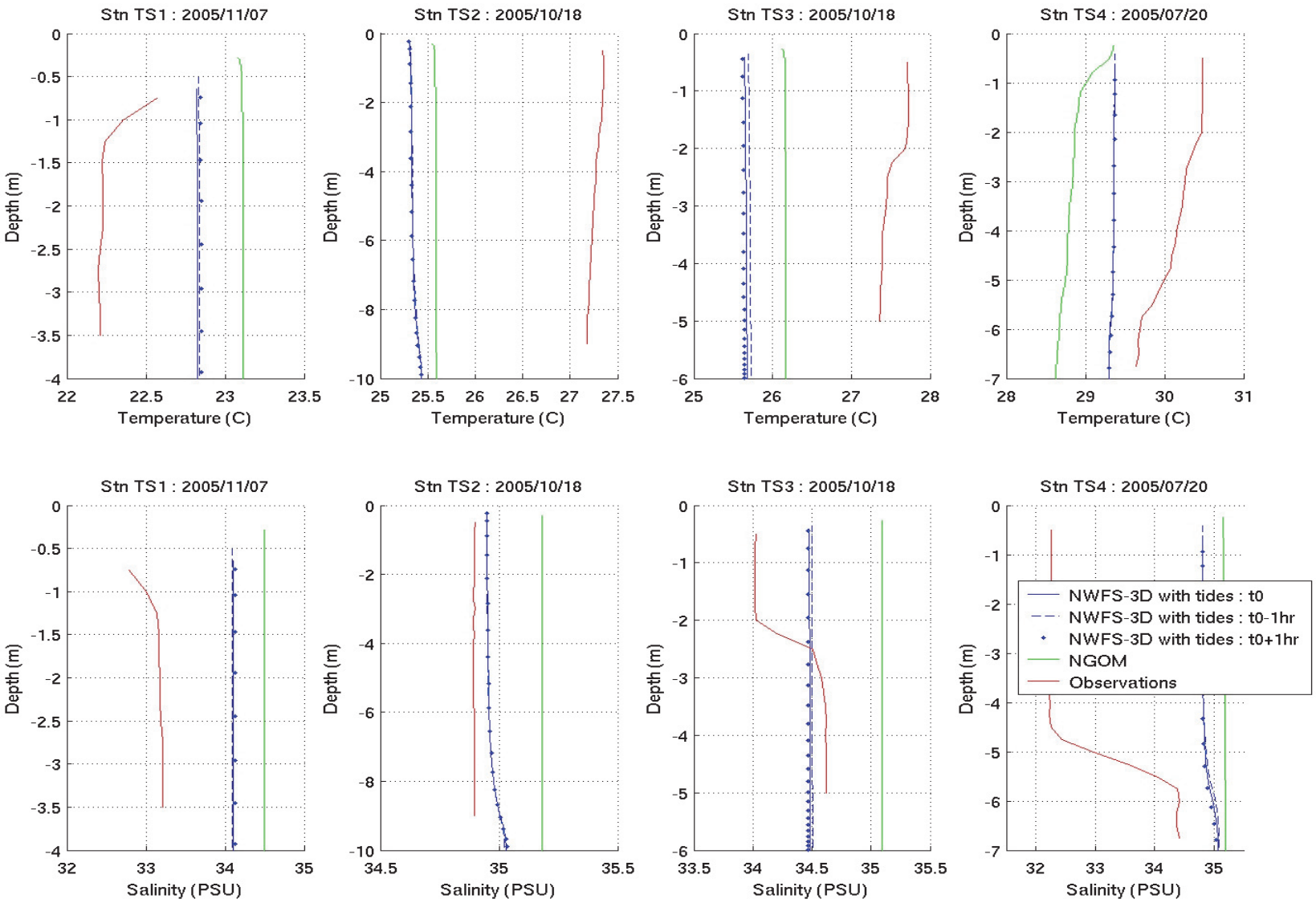

Figure B3. T/S vertical profile model-observation comparisons at stations TS1, TS2, TS3 and TS4.

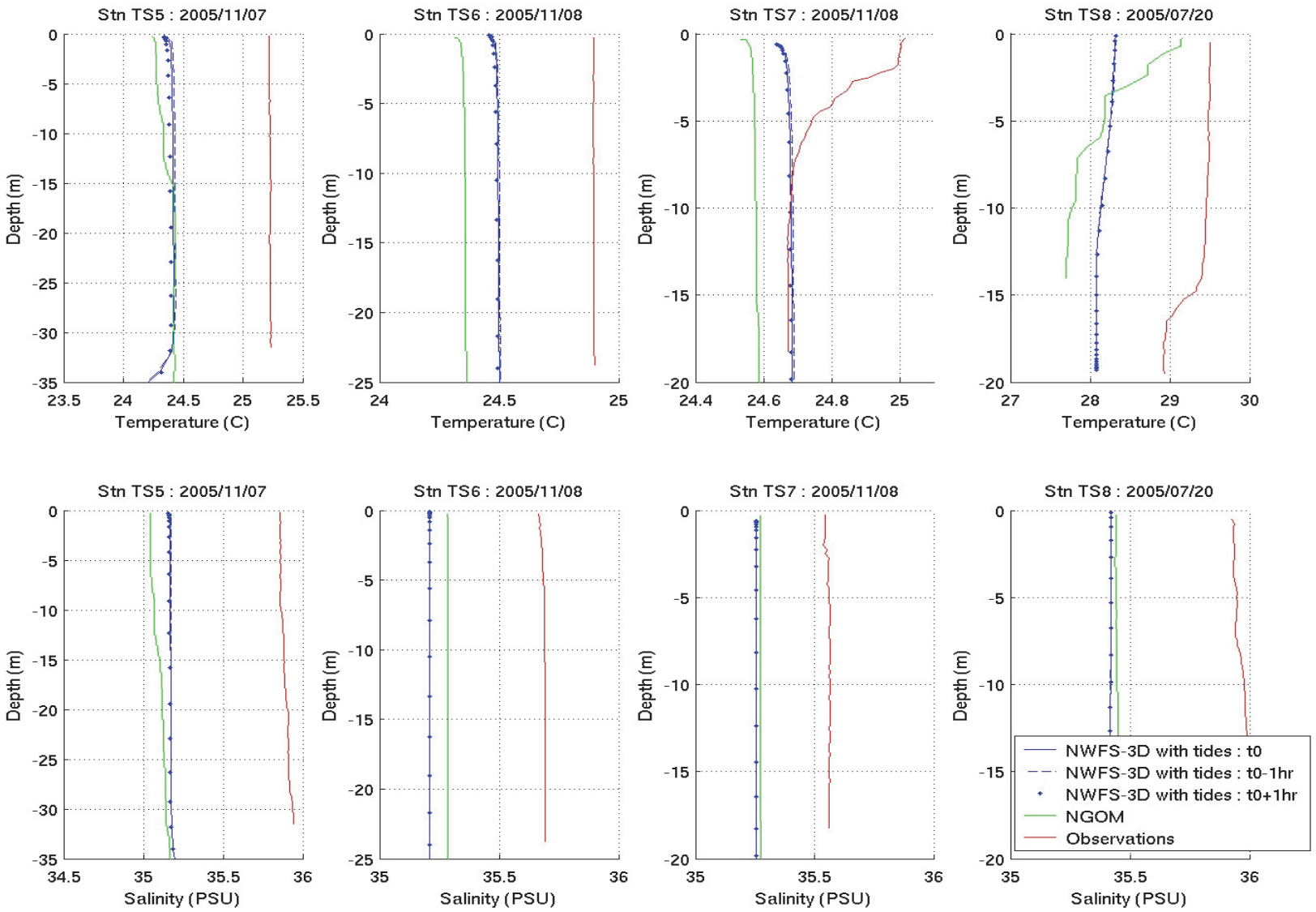

Figure B4. T/S vertical profile model-observation comparisons at stations TS5, TS6, TS7 and TS8.

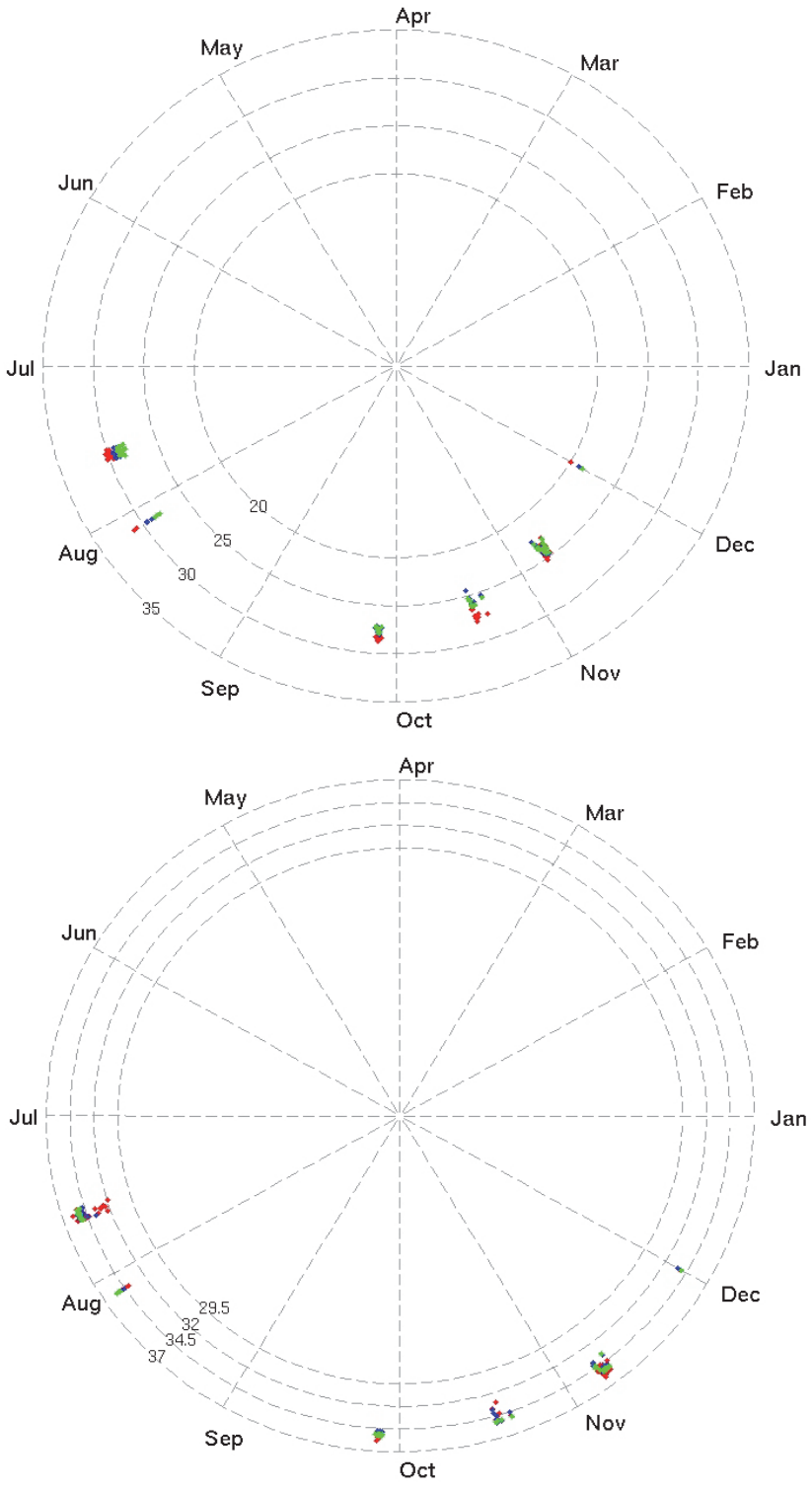

Figure B5. T (top, ^{o}C) and S (bottom, PSU) comparisons between NWFS-3D (blue), NGOM (green) and observations (red) at a 5m depth for 2005.

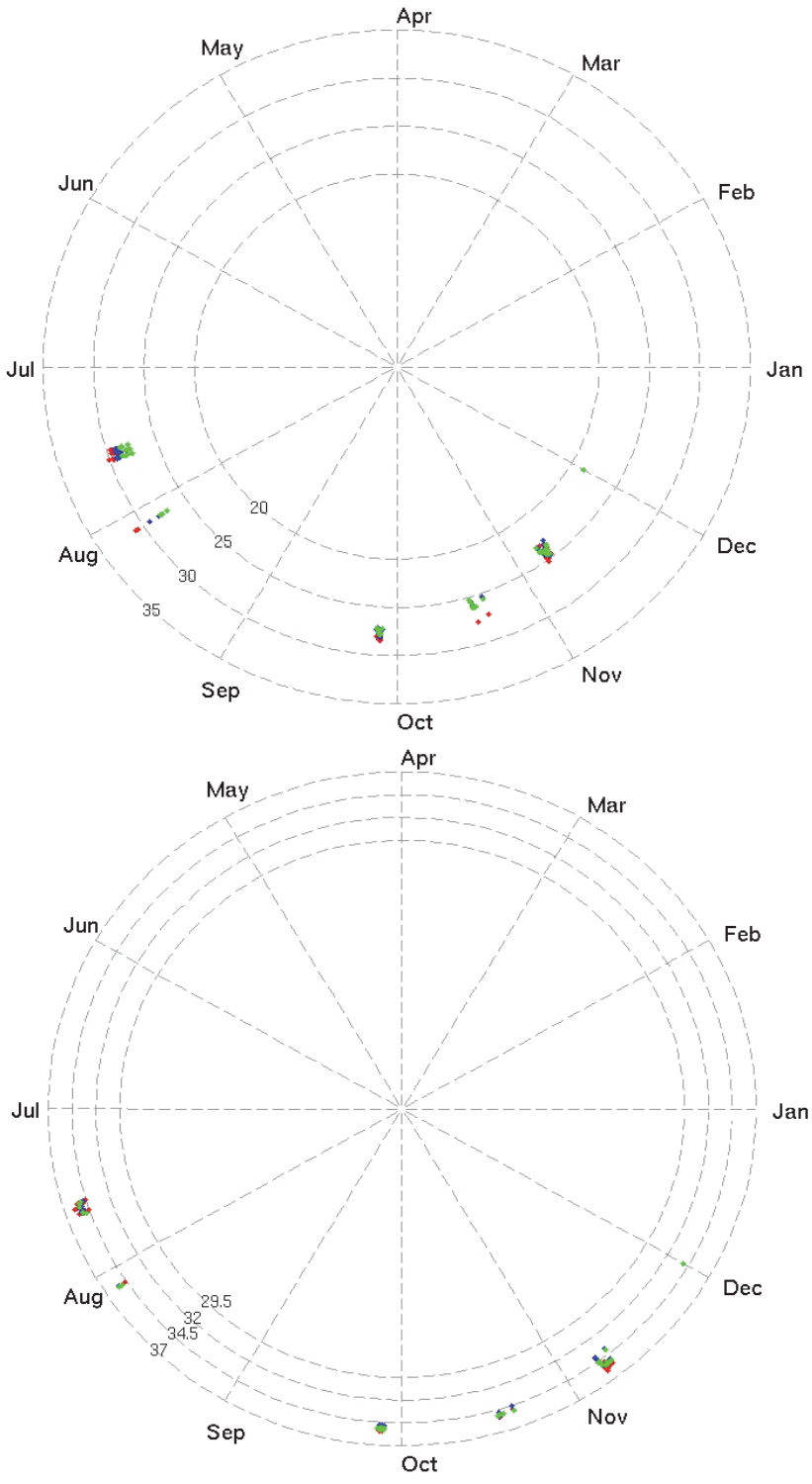

Figure B6. T (top, ^{o}C) and S (bottom, PSU) comparisons between NWFS-3D (blue), NGOM (green) and observations (red) at a 10m depth for 2005.

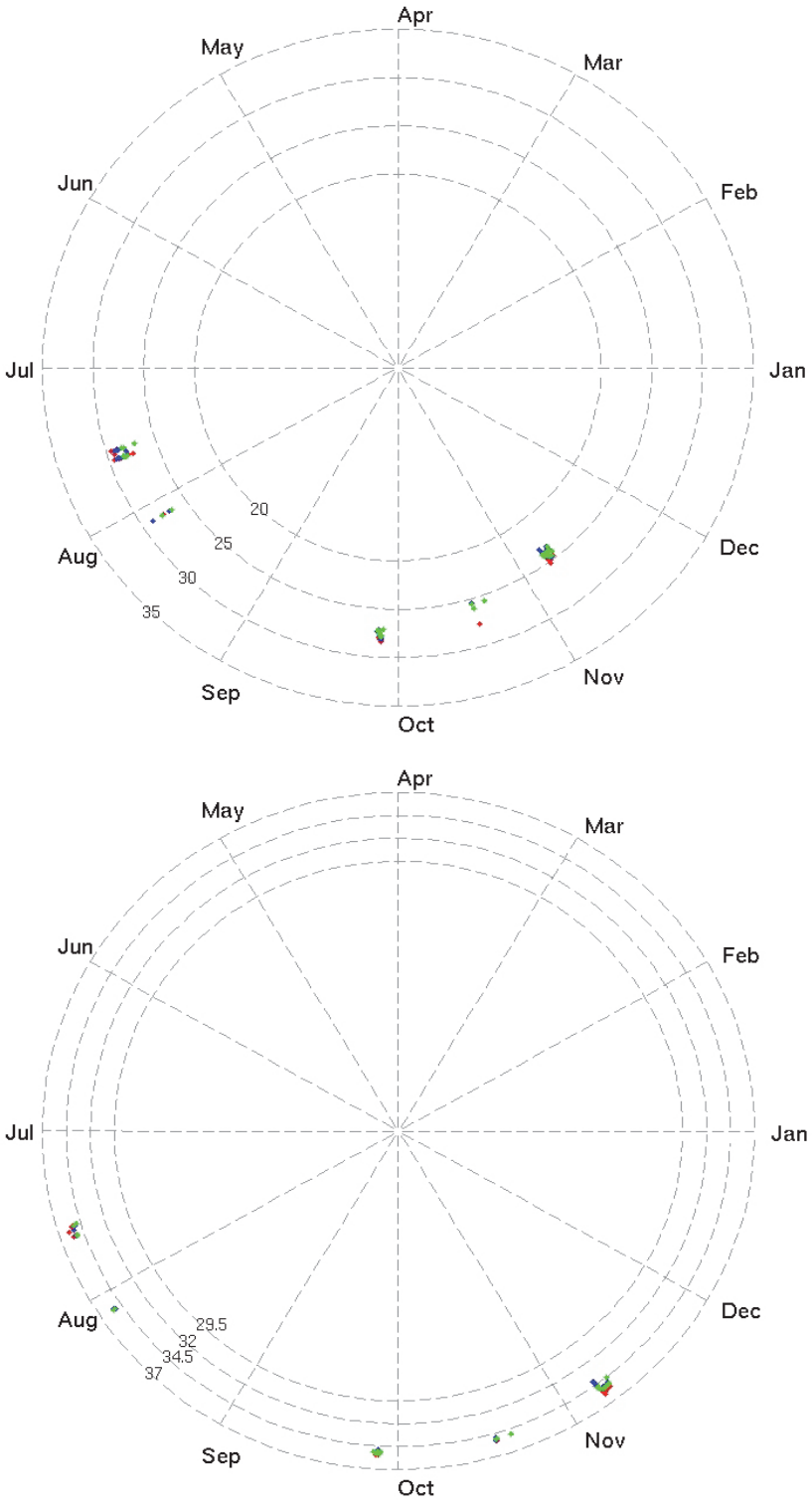

Figure B7. T (top, ^{o}C) and S (bottom, PSU) comparisons between NWFS-3D (blue), NGOM (green) and observations (red) at a 15m depth for 2005.